REPORT DOCUMENTATION PAGE

Form Approved OMB No. 0704-0188

1. AGENCY USE ONLY (Leave blank)	2. REPORT DATE	3. REPORT TYPE AND DATES COVERED
	28 January 2001	Technical Report, 12 Jun 00 – 28 Jan 01

4. TITLE AND SUBTITLE

Mechanism Of Beta-Grain Growth In Alpha/Beta Titanium Alloys During Continuous, Rapid Heating

5. FUNDING NUMBERS

N/A

6. AUTHOR(S)

Dr. Orest M. Ivasishin

7. PERFORMING ORGANIZATION NAME(S) AND ADDRESS(ES)

Institute for Metal Physics
36 Vernadsky Blvd
03680, Kiev 252142
Ukraine

8. PERFORMING ORGANIZATION REPORT NUMBER

N/A

9. SPONSORING/MONITORING AGENCY NAME(S) AND ADDRESS(ES)

EOARD
PSC 802 BOX 14
FPO 09499-0200

10. SPONSORING/MONITORING AGENCY REPORT NUMBER

STCU P-041

11. SUPPLEMENTARY NOTES

12a. DISTRIBUTION/AVAILABILITY STATEMENT

Approved for public release; distribution is unlimited.

12b. DISTRIBUTION CODE

A

13. ABSTRACT (Maximum 200 words)

Rapid Heat Treatment (RHT) of commercial titanium alloys is a promising novel technology ensuring a high level of mechanical properties as well as high cost efficiency of processing. One of the significant advantages of RHT is related to the possibility of employing heating to temperatures in the single-phase beta field. By this means, the technique can be used to obtain fully lamellar intragrain microstructures favorable for high creep resistance and fracture toughness with relatively small or moderate size beta-grains. Such microstructures give rise to good tensile ductility and fatigue properties, comparable to those of equiaxed or bimodal microstructures. Therefore, fully lamellar microstructures with a controlled beta grain size of around 100 micrometers are a feasible way to balance the tensile, fatigue, and creep properties of titanium alloys. With direct resistance heating, these microstructures and the corresponding properties can be produced throughout the part uniformly. With induction heating, gradient type microstructures can be produced in which the properties of surface and core volumes of the heat-treated part are selectively controlled depending on the intended service application. In either case, an understanding of beta grain growth behavior during continuous, rapid heating is the key point.

Thus, the goal of this investigation was to establish the temperature dependence of beta-grain size and its dependence on crystallographic texture for the alpha/beta alloy Ti-6Al-4V. The principal variables to be investigated include processing history, heating rate, and method of rapid heating (direct resistance or induction) in order to provide an explanation of beta-grain growth mechanism during continuous rapid heating. As a final output of this effort, practical recommendations for choosing RHT parameters to ensure optimized balance of mechanical properties will be developed.

14. SUBJECT TERMS

EOARD, Materials, Metallurgy & Metallography, Titanium

15. NUMBER OF PAGES

56

16. PRICE CODE

N/A

17. SECURITY CLASSIFICATION OF REPORT	18. SECURITY CLASSIFICATION OF THIS PAGE	19. SECURITY CLASSIFICATION OF ABSTRACT	20. LIMITATION OF ABSTRACT
UNCLASSIFIED	UNCLASSIFIED	UNCLASSIFIED	UL

SCIENCE AND TECHNOLOGY CENTER IN UKRAINE

INSTITUTE FOR METAL PHYSICS

EOARD

PARTNER PROJECT P-041

Mechanism of beta-grain growth in alpha/beta titanium alloys during continuous, rapid heating.

Final Report

Principal Investigator **Prof. O.M.Ivasishin**

Supervisor

Dr. S.L. Semiatin, AFRL

Kyiv-2001

Content

1. Introduction

Rapid Heat Treatment (RHT) of commercial titanium alloys is a promising novel technology which ensures a high level of mechanical properties as well as high cost efficiency of processing [1.1-1.3]. One of the significant advantages of RHT is related to the possibility of employing heating to temperatures in the single-phase beta field. By this means, the technique can be used to obtain fully lamellar intragrain microstructures favourable for high creep resistance and fracture toughness with relatively small or moderate size β-grains. Such microstructures give rise to good tensile ductility and fatigue properties, comparable to those of equiaxed or bimodal microstructures [1.1-1.4]. Therefore, fully lamellar microstructures with a controlled beta grain size of around 100 μm are a feasible way to balance the tensile, fatigue, and creep properties of titanium alloys. With direct resistance heating, these microstructures and the corresponding properties can be produced throughout the part uniformly.

The duration of the RHT must be carefully controlled to prevent excessive grain growth. Hence, an understanding of grain growth phenomenology of a single-phase alloys is important for the design and control of RHT processes to produce controlled microstructures.

Several studies have been conducted to establish the kinetics of beta grain growth for both conventional, long time (furnace) and short time (salt pot, induction) heat treatments [1.4-1.8]. A comparison of the results of various studies reveals deviations from the classical normal grain growth kinetics whose physical reasons have not yet been clarified.

The normal *isothermal* grain growth kinetics can be expressed by the classical grain growth equation:

$$D^n = \mathrm{Kt}\exp(-Q/R\mathbf{T}), \tag{1}$$

or,

$$D^n - D_0^n = \mathrm{Kt}\exp(-Q/R\mathbf{T}); \tag{2}$$

in which Q is the activation energy; D and D_0 denote the initial and final grain sizes; t is the annealing time; R is the gas constant; $\mathbf{T}$ is the absolute temperature; n is the grain growth exponent, and K represents the rate constant. Exponential part of the equations (1, 2) comes from the temperature dependence of the boundary mobility [1.9] which is closely related to a local diffusion process near to or in the moving interface and can be given by the Arrhenius equation:

$$M(\mathbf{T}) = M_0 \exp(-Q/R\mathbf{T}), \tag{3}$$

where, M_0 is the pre-exponential factor.

Equations (1) and (2) allows n and Q to be found by using experimental data on isothermal grain growth. The grain growth exponent n is proportional to the slope of the $\ln D$ vs. ln t graph, and Q can be evaluated from the slope of $\ln D$ vs. ln $(1/\mathbf{T})$ graph, taking into account that:

$$Q/nR = -(\ln D) / (\ln (1/\mathbf{T})). \tag{4}$$

When n and Q values are known, K value can be determined using the fitting procedure to the experimental data. An example of the lg$D$ vs. lg t graphs taken from [1.7] is presented at Figure 1.1. It should be mentioned that this approach is correct for a relatively big D values.

For grain growth during a *continuous heating* characterized by a constant heating rate, $\dot{\mathbf{T}} = d\mathbf{T}/dt$, equation (2) may be converted into a simple differential equation that is readily integrated to yield the following expression for grain size as a function of $\dot{\mathbf{T}}$, the initial and final temperatures, $\mathbf{T}_i$ and $\mathbf{T}_f$, respectively, and the material coefficients n, K, and Q, if it is assumed that n, K, and Q are independent of temperature [1.8]:

$$D^n - D_0^n = (KR/\dot{\mathbf{T}}\,Q)\{[\mathbf{T}_f^2 \exp(-Q/R\mathbf{T}_f)] - [\mathbf{T}_i^2 \exp(-Q/R\mathbf{T}_i)]. \quad (5)$$

Two approaches were developed in [1.4, 1.5, 1.10] to find the n, K, and Q values. First is fully based on set of experimental data on grain growth during continuos heating with constant rates $\dot{\mathbf{T}}_1, \dot{\mathbf{T}}_2, \dot{\mathbf{T}}_3, \ldots$. For fixed values of $\mathbf{T}_i$ and $\mathbf{T}_f$ and $D >> D_0$, equation (5) yields the following relationships for n and Q:

$$n = (-d\log D/d\log \dot{\mathbf{T}})^{-1}; \quad (6)$$

$$Q = R[\ln(\dot{\mathbf{T}}_2/\dot{\mathbf{T}}_1) - 2\ln(\mathbf{T}_{f1}/\mathbf{T}_{f2})] \bullet (1/\mathbf{T}_{f1} - 1/\mathbf{T}_{f2})^{-1}. \quad (7)$$

The value of K can be than found using standard fitting procedure. Example of the n, K, and Q evaluation by using the above approach is presented on Figure 1.2 [1.4], which shows a reasonably good fit between model and experiment. Some discrepancy between the beta grain growth modeling, based an equations (6) and (7) and experimental values of average beta grain size exists, however, at relatively high temperatures at which the beta grains grow to about 200 micrometer size (calculated sizes were higher than those obtained experimentally). One explanation of this is that beta-grain growth during continuous rapid heating may be controlled not only by thermally activated boundary movement but also by the development of beta-phase texture.

Second approach to material coefficients estimation [1.5] consists in using of a numerical procedure based directly on equation (1). In this method, a wide range of combinations of n, K, and Q values are inserted into (1), which was than numerically integrated for each of the experimental heating rates $\dot{\mathbf{T}}$ from $\mathbf{T}_i$ to $\mathbf{T}_f$ using small time increments of $0.5^{\circ}\mathrm{C}/\dot{\mathbf{T}}$ in order to predict D as a function of temperature $\mathbf{T}$. The best set of material coefficients is determined as that for which the average (absolute) percentage deviation between the measurements and predictions is least.

As reviewed in [1.9], texture may have a substantial influence on grain growth via its effect on grain boundary energy and mobility M_0. The essential texture effects during isothermal beta grain growth in titanium alloys were assumed in [1.7, 1.8]. The influence of crystallographic texture on the beta grain growth kinetics during continuous heating in Ti-6Al-4V was studied in [1.10]. To evaluate the material coefficients n, K, and Q, the first approach based on equations (6) and (7) was

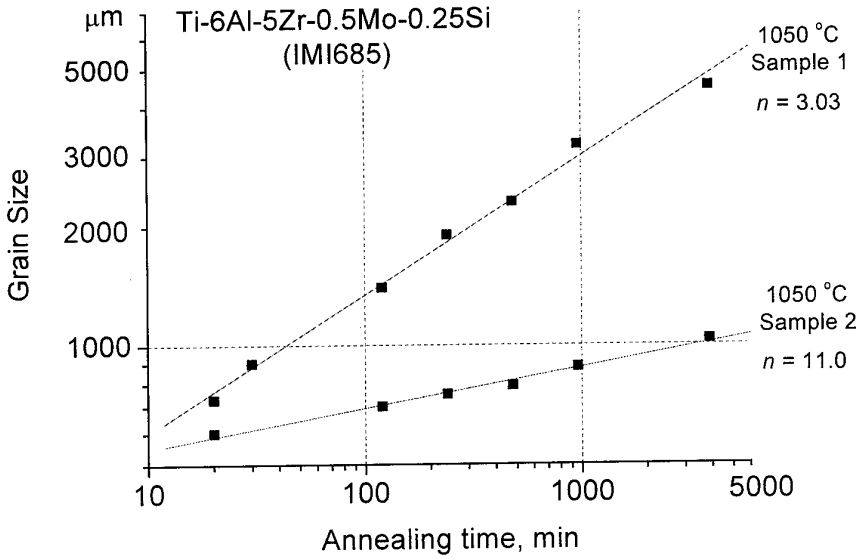

Figure 1.1. Examples of lg D vs. lg t graphs for samples exhibiting normal (n=3.03) and slow (n=11.0) grain growth in the material having the same chemical composition [1.7].

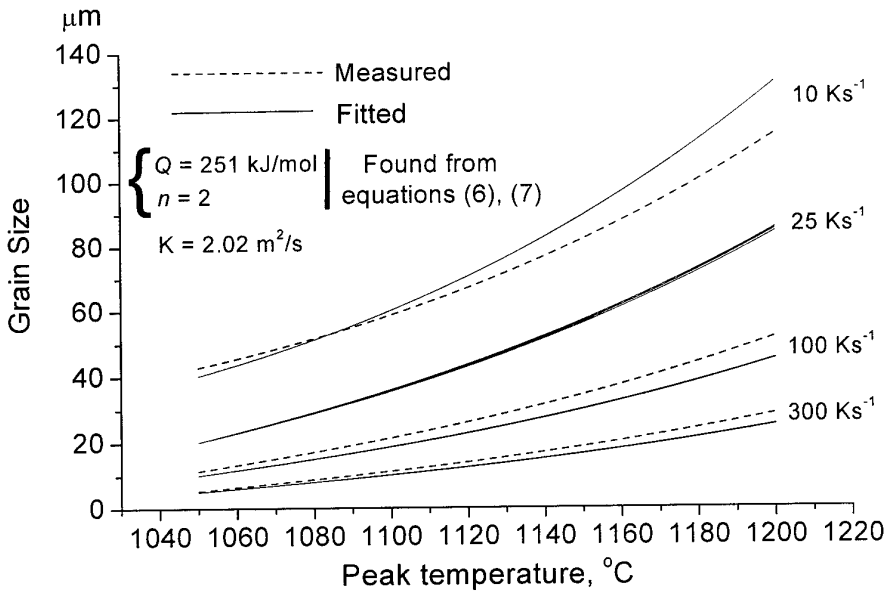

Figure 1.2. Fitting the beta grain growth model predictions [1.10] to the experimental data [1.11] for VT9 alloy.

used. Two lots of Ti-6Al-4V material having in as-received state essentially different textures of beta phase were continuously heated with $\dot{T}$ = 1.39, 5.56 and 17.9 Ks^{-1} to peak temperatures between 1300 and 1535 K. One lot developed much smaller beta grain sizes than the other for a given set of processing conditions. A semi-quantitative analysis of the results revealed that the two batches of alloy had similar grain-growth exponents n and activation energies Q but different rate constants K. Since one material had a moderate strength, cube-like texture, whereas the other exhibited a very strong and sharper fiber texture. The grain-growth results were thus explained in terms of the effect of texture on grain-boundary surface energy/mobility (development of a sharp texture of high intensity early in the beta annealing process appeared to be the source of slower grain growth).

Due to several reason, paper [1.10] remained many aspects of texture influenced grain growth under the question: (1) chemical compositions and microstructure of two lots ofTi-6Al-4V were not identical. This implies that different grain growth behavior of two lots could be, at least partly, related to the chemistry, for example to a different influence of solute drag effect; (2) the assumption that material coefficients n, K, and Q are constants with temperature might be correct; (3) evolution of beta phase texture during grain growth was supposed only from texture of alpha phase formed via $\beta \rightarrow \alpha$ transformation on cooling; (4) temperature dependencies of beta grain size where not thorough since they were based on three peak temperatures.

The goal of present investigation was to carefully establish the temperature dependencies of beta-grain size in alpha/beta alloy Ti-6Al-4V for two materials that differ *only* in their crystallographic texture in order to develop the phenomenological approach to the beta grain growth in titanium alloys that includes the effect of texture evolution on grain growth kinetics.

References.

1.1. Gridnev V.N., Ivasishin O.M., Oshkadjorov S.P. Physical Principles of Rapid Heat Treatment of Titanium Alloys, (in Russian), Kyiv, Naukova Dumka Publish., 1986, 346 p.

1.2. Ivasishin O.M., Markovsky P.E. Enhancing the Mechanical Properties of Titanium Alloys with Rapid Heat Treatment (Overview), JOM, 1996, #7, pp.48-52.

1.3. Semiatin S.L. and Sukonnik I.M. Rapid Heat Treatment of Titanium Alloys, In: Proc. Of 7th International Symposium on Physical Simulation of Casting, Hot Rolling and Welding, 21- 23.01.1997, ISPS. pp. 295-405.

1.4. Semiatin S.L., Soper J., and Sukonnik I.M., Short -Time Beta Grain Growth Kinetics for a Conventional Titanium Alloy, Acta Mater., 44, #5, (1996), pp.1979-1986.

1.5. Semiatin S.L., Soper J., and Sukonnik I.M., Scripta Metall. et. Mater., 1994, #30, pp. 951-958.

1.6. Ivasishin O.M., Markovsky P.E., Wagner L., and Lutjering G., in Titanium 1990:Products and Applications. Titanium development Association, Dayton, OH, 1990, pp.99-110.

1.7. Fox S.P. A Study of Grain Growth Behavior in Titanium Alloys. Proc. of Titanium'92, Science and Technology, ed. Froes F.H. and Caplan I.L. 1992, pp.769-776.

1.8. Gil F.J., Tarin P. and Planell J.A. Grain Growth Kinetics in Beta Phase ofTi-6Al-4V Alloy. Proc. of Titanium'92, Science and Technology, ed. Froes F.H. and Caplan I.L. 1992, pp. 777-784.

1.9. Gordon, P. Energetics in Metallurgical Phenomena, Vol. 1, Gordon and Breach, New York, 1962,p.207.

1.10. Semiatin S.L., Fagin P.N., Glavicic M.G, Sukonnik I.M., and O.M. Ivasishin. Influence of Texture on Beta Grain Growth During Continuous Annealing of Ti-6A1-4V. Mat. Sci. And Eng., V. A299, 2001, pp. 225-234.

1.11. Bodyako M.N., Gordienko A.I., Elagina L.A., and Ivashko V.V. in Titanium, Science and Technology ed. G. Lutjering, U. Zwicker, and W. Bunk. Deutche Gesellschaft fur Metalkunde e.V. Oberrursel, Germany, 1984, pp. 1621-1628.

2. Thermomechanical processing of Ti-6Al-4V to produce texturally different but morphologically equivalent equiaxed microstructures.

Commercial alpha + beta alloy Ti-6Al-4V, which is a "working horse" of world titanium industry, was chosen as most typical representative of structural titanium alpha+beta alloys. Two Ti-6Al-4V as-received materials of nearly equivalent chemical composition (Table 2.1) were first tried in this study: round cross-section ∅ 25 mm bar and 16 mm thick plate.

Table 2.1. Chemical composition of studied Ti-6Al-4V materials.

	Content of alloying elements, wt.%				
	Al	V	Fe	Mo	Ti
Bar	5.98	4.25	0.17	0.05	Balance
Plate	6.05	4.40	0.15	0.02	Balance

Keeping in mind project goal, following *requirements to preparation of starting material* were formulated: (1) Two chemically and morphologically equivalent, but texturally different microstructures should be prepared and (2) microstructures should be of equiaxed type and as fine and uniform as possible;

Reason for the last requirement is following. It is well known that geometry of alpha phase is a main factor defining alloy behavior upon rapid heating, specifically, the beta-transus temperature T_β at given heating rate [2.1]. Coarser alpha particles in starting microstructure cause in bigger shift of T_β to higher temperatures with heating rate increase. In case when the microstructure of titanium mill products varies significantly from one location to another (alpha particles of different geometry are present simultaneously) like it was in as-received material (Figure 2.1) the end of polymorphous transformation will be controlled by transformation of the *largest* α grain even though a single-phase β microstructure may form earlier in other regions. This may give rise to a grain-size nonuniformity after rapid heating because grain growth may not begin simultaneously in all areas of the part. Therefore, it was aimed in present study that the initial microstructure should be the finest possible and uniform to minimize an influence of heating rate on T_β temperature, which, in turn, determines a starting point of beta-grain growth.

The above requirement to the starting microstructure was ensured using thermomechanical approach based on a relatively strong deformation (rolling) of preliminary beta solutioned and forced cooled material followed by (α+β) recrystallization annealing (Figure 2.2). It was shown in [2.2] that one can get various by changing temperature of deformation textures while temperature of annealing defines dispersion of resulting α+β microstructure. In this approach, prior beta solutioning is an important step aimed to eliminate an influence of as-received microstructure and texture

on a resultant features of rolled product since primary alpha phase is fully dissolved and fine lamellar type microstructure forms (Figure 2.3). Rolling was done in two roller mill at temperatures 800, 850 and 900°C. Reduction degree varied in 60-90% range: number of passes varied from 3 to 8 to obtain different "stiffness" of deformation. Recrystallization annealing aimed to form homogeneous equiaxed $\alpha+\beta$ microstructure was done at 850°C, 1h.

Experiments showed that most uniform equiaxed microstructure with average α grain size of 2-3 μm (Figures 2.4) could be achieved employing not less than 80% reductions at 850°C. Deformation at 800°C did not allow to reach higher than 70% reduction without material cracking, which was not enough to avoid a formation of higher than unity aspect ratio alpha phase (Figure 2.5). Rolling at 900°C was accompanied by a selective dynamic recrystallization resulting in coarser and less uniform microstructure. There was no obvious difference between bar and plate materials in their microstructural response to the above thermomechanical processing as well as between materials rolled with different number of passes (compare Figure 2.4a and b). This allowed to conclude that rolling temperature and reduction degree are two major parameters controlling dispersion and uniformity of final microstructure.

Texture analysis showed that the as-received materials were only weakly textured. The texture of as-received bar was very weak while the texture of the as-received plate was inhomogeneous through the thickness. Solid solutioning prior to rolling caused in elimination of initial textures and formation of random texture imposed by $\beta\rightarrow\alpha$ phase transformation. Isothermal rolling at 850°C with total reduction degree of 80% and low reductions at each rolling pass (about 10%) formed basal type alpha phase texture while isothermal rolling at the same temperature with 87% total reduction and high reductions at each rolling pass led to a formation of basal-transverse texture of alpha phase (Figure. 2.6).

The textures of alpha phase produced by rolling were generally sharper in case of starting plate material, therefore further experiments were conducted with this particular material. Based on the above results two batches of materials having equivalent chemistry and microstructure (Figure 2.4 a and b), but different crystallographic textures of alpha phase (specifically, basal and basal-transverse) were obtained. First was processed by rolling at 850°C from 16 to 5 mm in 8 rolling passes; second one was processed by rolling at the same temperature from 16 mm to 2 mm in 4 rolling passes. Because of a difference in final thickness the materials are thereafter called plate material (PM) and sheet material (SM) respectively.

Textures of beta phase in PM and SM are presented in Figure 2.7. Pole figures $(100)_\beta$ for PM and SM are generally of the same type, much sharper in SM, which comes from recovery and partial recrystallization of typical for b.c.c. metals rolled components and corresponding spreading of orientations. It should be mentioned that texture analysis of beta phase in Ti-6Al-4V is rather difficult experimental procedure, first of all, because of low volume fraction of the beta phase (being less than 10%). Moreover, the $(110)_\beta$ peak with the highest structural factor is close to $(0002)_\alpha$ and $(1011)_\alpha$ peaks, which typically have high intensity. To avoid overlapping of stronger reflections of alpha and weak beta peaks, vertical aperture having horizontal resolution not more than 0.25° in a θ

direction was placed in front of detector. Divergency of primary X-ray beam was reduced using graphite monochromator and system of apertures forming spot on the specimen surface 0.5 x 0.5 mm that eliminated peak widening at specimen tilting. Averaging of texture inhomogeneity was done by linear scanning along the specimen. To improve the signal to noise ratio the measuring time was increased.

References

2.1 Gridnev V.N., Ivasishin O.M., Markovsky P.E. Influence of heating rate on the temperature of the $\alpha+\beta\rightarrow\beta$ transformation of titanium alloys, Metal Science and Heat Treatment, V.25, (1-2), 1985, pp.43-47.

2.2 Luetjering G, Peters M., Mechanical Properties of a Titanium Blading Alloy, EPRI CS-2933 Research Project 1266-1, final report, Hamburg, 1983, 110 pp.

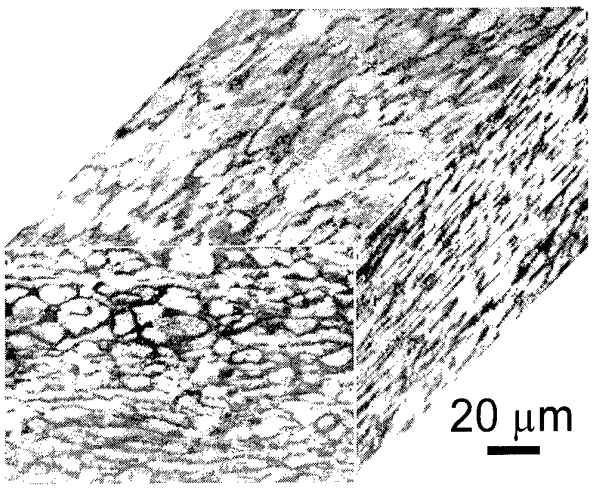

Figure 2.1. 3D microstructure of as-received Ti-6Al-4V plate. LM

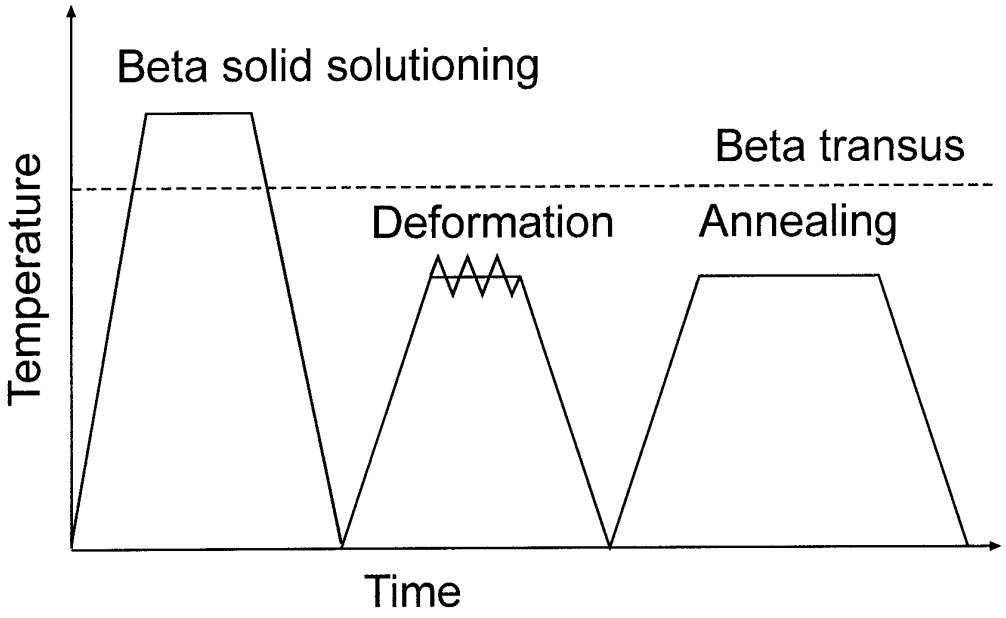

Figure 2.2. Scheme of thermomechanical processing employed to obtain fine uniform microstructures.

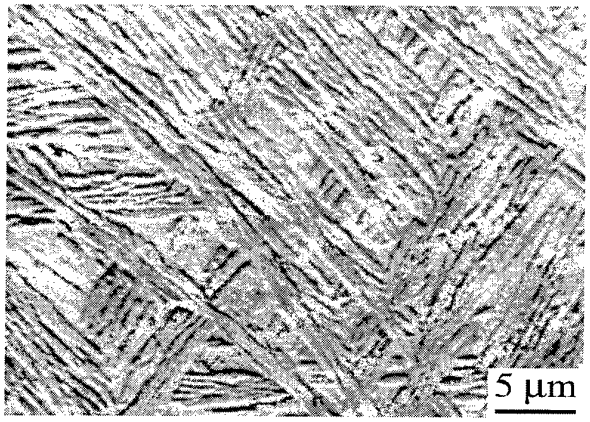

Figure 2.3. Microstructure of Ti-6Al-4V after solid solutioning at1100°C, 0.5h followed by forced cooling. LM

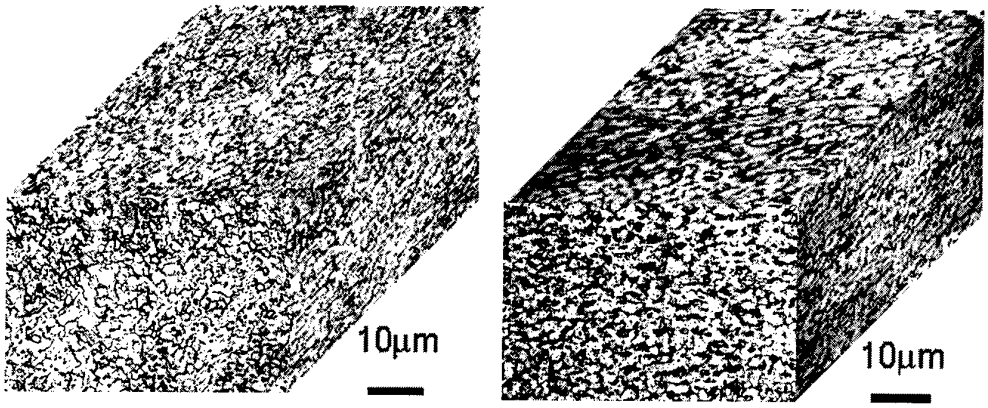

a)

b)

Figure 2.4 3D microstructure of Ti-6Al-4V plate processed as on Figure 2.2. Reduction on rolling: (a) 80% in 8 passes, (b) 87% in 4 passes. LM

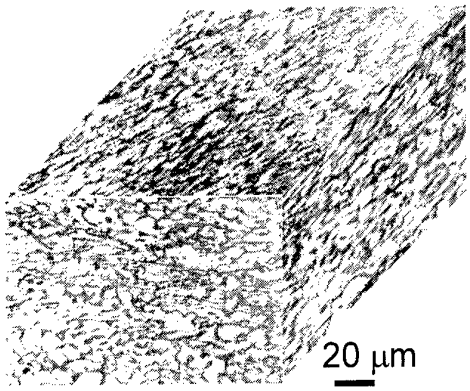

Figure 2.5. 3D microstructure of Ti-6Al-4V plate processed as on Figure 2.2. Reduction on rolling 60% in 8 passes.

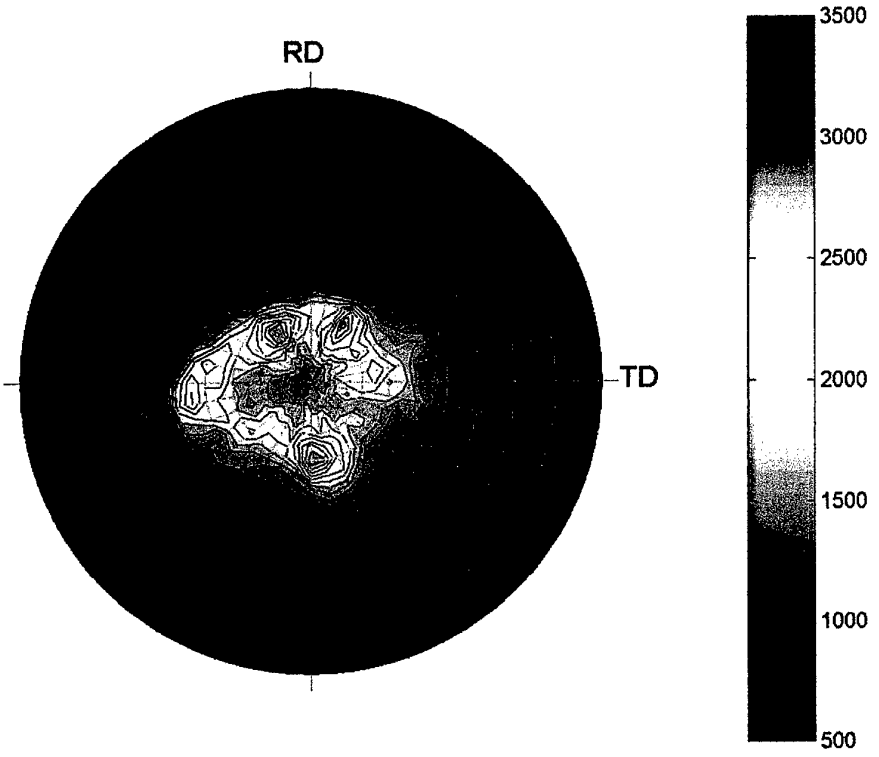

a)

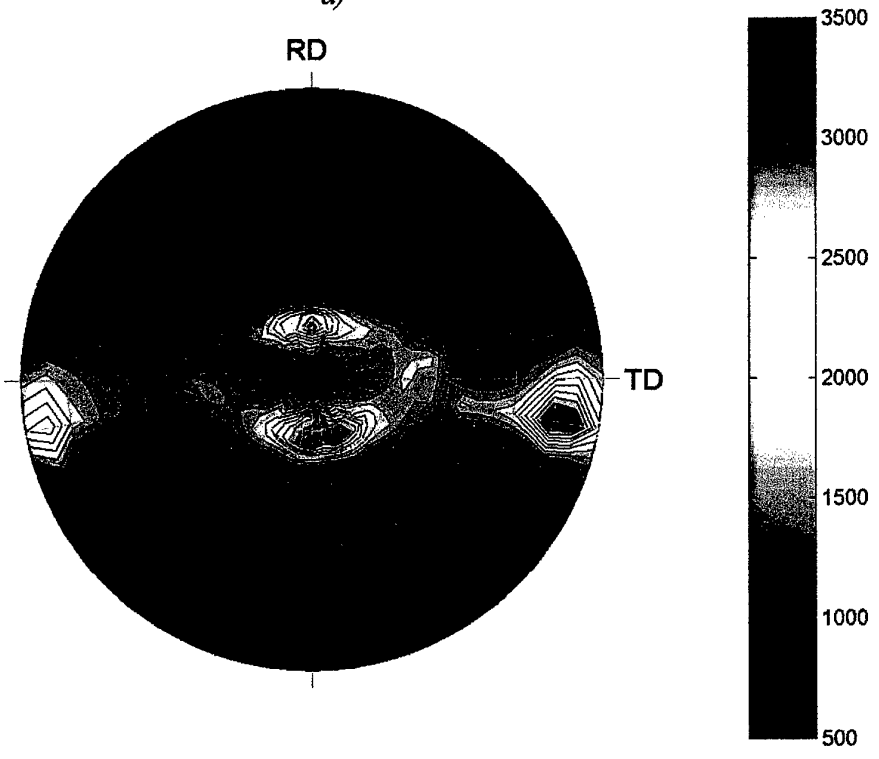

b)

Figure 2.6. (0002) alpha phase pole figures of (a) PM and (b) SM.

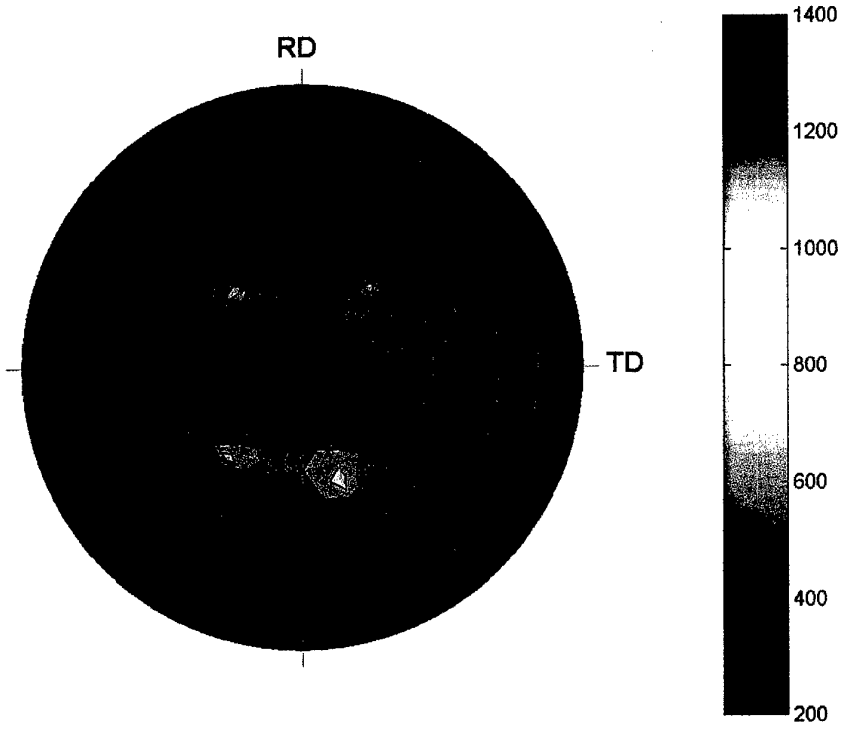

a)

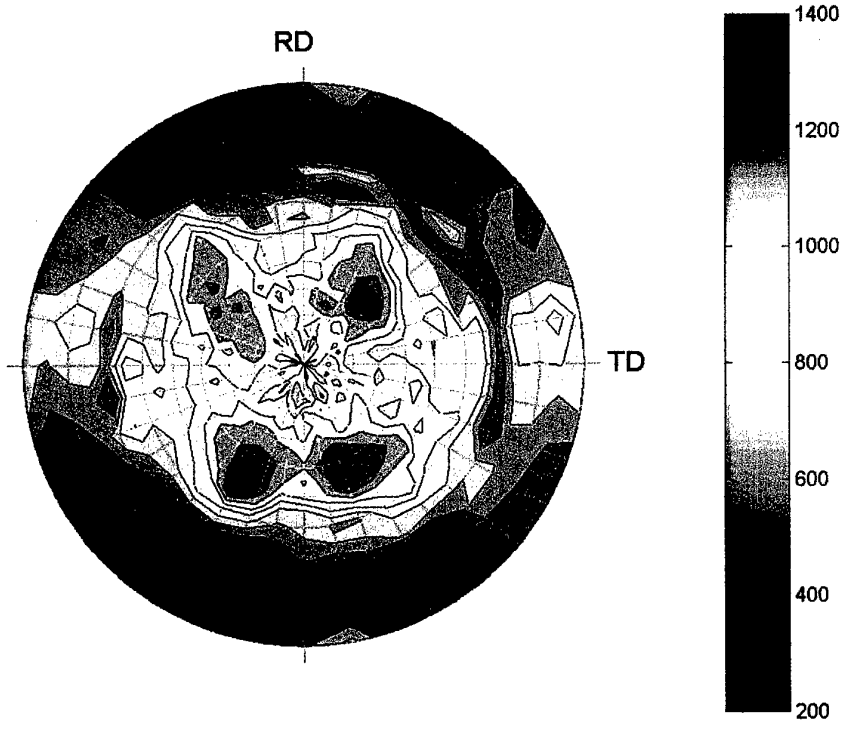

b)

Figure 2.7. (110) beta phase pole figures of (a) PM and (b) SM

3. Grain growth and texture evolution at continuous heating.

Rapid continuous heating with heating rates of 0.42, 5, 10, 20 and 50 Ks^{-1} to various temperatures within beta field with a small temperature increment was performed using direct electric resistance technique (50 Hz). After reaching specified temperature specimens were rapidly cooled to retain beta grain size achieved on heating.

Heating rate dependence of beta-transus temperature T_β, that should be also considered as starting temperature of beta grain growth, was determined (Figure 3.1.) using "in situ' thermo-resistometric method and verified by LM examination. As it is seen from Figure 3.1, both PM and SM, due to equivalency of their microstructures have equivalent beta-transus temperatures at any heating rate investigated. This proves that for equivalent morphologies, heating rate dependencies of T_β are similar *irrespective* of alpha phase texture and provides an equal starting conditions for beta grain growth in SM and PM. It should be mentioned that due to high uniformity of both microstructures, they have quite narrow range of T_β variation from one location to another. In turn, this allows to determine more precisely the initial temperature T_i of beta grain growth and initial beta grain size D_i. For comparison, on the same Figure 3.1 the data for coarser microstructure (as-received plate) are presented which confirm an essential role of alpha phase geometry on the beta-transus temperature at rapid heating, well established earlier [3.1, 3.2].

Typical example of beta grain evolution during continuous rapid heating above T_β temperature is presented in Figure 3.2. Microstructural images of rapidly heated specimens were treated by means of the quantitative metallography using linear intersections method and "IMAGE-PRO" software. Experimental results for SM and PM plotted as "beta-grain size vs. peak temperature" dependencies for the above mentioned heating rates (Figures 3.3 and 3.4). It can be clearly seen that, in general, beta grain growth doesn't correspond to exponent law as it could be expected from earlier publications and modeling. The grain growth occurs faster for PM, i.e. for material with weaker texture. For instance, after heating 5 Ks^{-1} to 1250°C the beta-grain size is 200 μm in SM and 250 μm in PM. Even more pronounced is this effect for heating rate 0.42 Ks^{-1}.

More careful analysis of continuous heating grain growth data by comparing grain sizes achieved in SM and PM at equivalent heating rates of 0.42, 5 and 50 Ks^{-1} (Figure 3.5) shows that at a relatively low beta temperatures the dependencies follow the same line splitting only after temperature exceeds some specific value, the last increasing with heating rate increase and being 1040°C, 1100°C and 1150°C for heating rates 0.42Ks^{-1}, 5Ks^{-1} and 50 Ks^{-1} respectively. Only after the splitting beta grains grow slower in SM. Since two materials are differ in crystallographic texture only, key role of texture in this phenomenon becomes obvious. However, texture begins to affect grain growth only on some stage of grain growth. In order to understand such a behavior beta phase texture evolution during rapid heating in single-phase beta field was analyzed.

It is worth to note that in material like Ti-6Al-4V direct determination of high-temperature beta-phase texture has not been performed earlier since under rapid cooling from peak temperature beta phase undergoes complete transformation with no residual phase remained. Beta phase partially remains at slower cooling rates when diffusional

type $\beta \rightarrow \alpha+\beta$ transformation occurs. Such cooling, however, does not prevent beta grains from further growing. The problem was solved by using special cooling procedure (Figure 3.6): after reaching peak temperature specimen was cooled with a rate of about 300 Ks^{-1} to around 800°C (above M_S temperature) to prevent an additional grain growth, then exposed at this temperature during 5 minutes to ensure diffusional decomposition of beta phase and, finally, air-cooled to room temperature. This allowed to get 6 to 8% of residual beta phase for texture measurement. Control experiments showed that specimens cooled directly to room temperature or via the above regime had actually the same beta-grain microstructure.

Evolution of beta-phase texture in SM during continuous heating in single-phase beta field is well seen from Figures 3.7 on which data for heating rate 10 Ks^{-1} are presented at a relatively small temperature increment. By the end of $\alpha+\beta \rightarrow \beta$ transformation (1000°C) the texture remains of the same type as the initial one (see Figure 2.8) except that components {110} <211> and {001} <110> are not more resolved. However, very soon, at 1050-1100°C well defined orientation distribution changes toward a random one. The most striking result follows from analysis of pole figure corresponding to 1150°C, which shows that material again becomes well textured (!). The temperature at which it happens is very close to that at which beta grain growth in SM is slowing down. At 1200°C and above the random orientational distribution was again observed. It should be noted, however, that results on texture of beta phase at high temperatures are not quite reliable because of coarsening of grain structure. With an increase in heating rate to 50 Ks^{-1}, SM did not any sign of texturing up to highest temperatures investigated (1150°C, Figure 3.8). The "secondary" texturing was not observed in PM neither at 10 Ks-1 nor at 50 Ks-1 heating rates (Figure 3.9).

Induction heating

Experiments on induction heating were done using 7 kHz generator having power capacity of 5 kW. Flat loop inductor was used as a heating element placed above surface of the same specimens as those used for electric resistance heating. Control thermocouple was welded to surface and calked trying to avoid influence of whirling currents. Varying power output and air clearance, heating rates in the range 10-80 Ks^{-1} were reached.

Typical example of microstructure formed through the cross section of PM is presented in Figure 3.10. The gradient type of microstructure is clearly seen, which is due to a heat generation in comparatively thin surface layer followed by heat transfer into deeper locations. Being useful when combination of properties different for rim and core areas are necessary [3.3], the induction heating method was considered as inappropriate for this study since it needs very careful layer-by-layer measurements and modeling to find out an adequate relationship between heating parameters and effects. Some experiments which need 3D analysis, for instance, texture evolution measurements would be impossible in induction heating technique.

References

3.1. Gridnev V.N., Ivasishin O.M., Oshkadjorov S.P. Physical Principles of Rapid Heat Treatment of Titanium Alloys, (in Russian), Kyiv, Naukova Dumka Publish., 1986, 346 p.

3.2. Gridnev V.N., Ivasishin O.M., Markovsky P.E. Influence of heating rate on the temperature of the $\alpha+\beta\rightarrow\beta$ transformation of titanium alloys, Metal Science and Heat Treatment, V.25, (1-2), 1985, pp.43-47.

3.3. Semiatin S.L. and Sukonnik I.M. Rapid Heat Treatment of Titanium Alloys, In: Proc. Of 7th International Symposium on Physical Simulation of Casting, Hot Rolling and Welding, 21- 23.01.1997, ISPS. pp. 295-405.

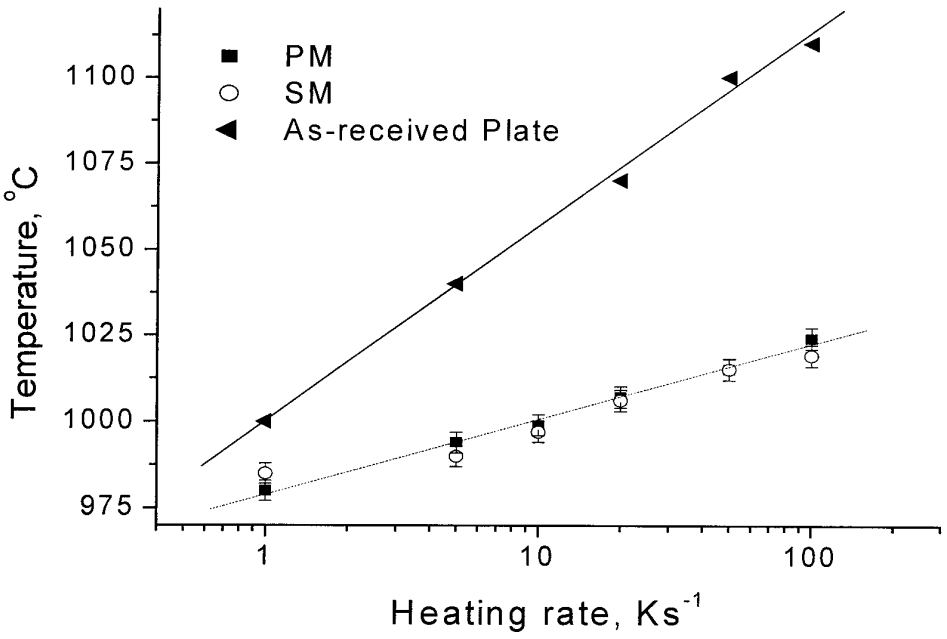

Figure 3.1. Heating rate dependence of beta transus temperature for: (O) SM, (■) PM and (◂) as-received plate.

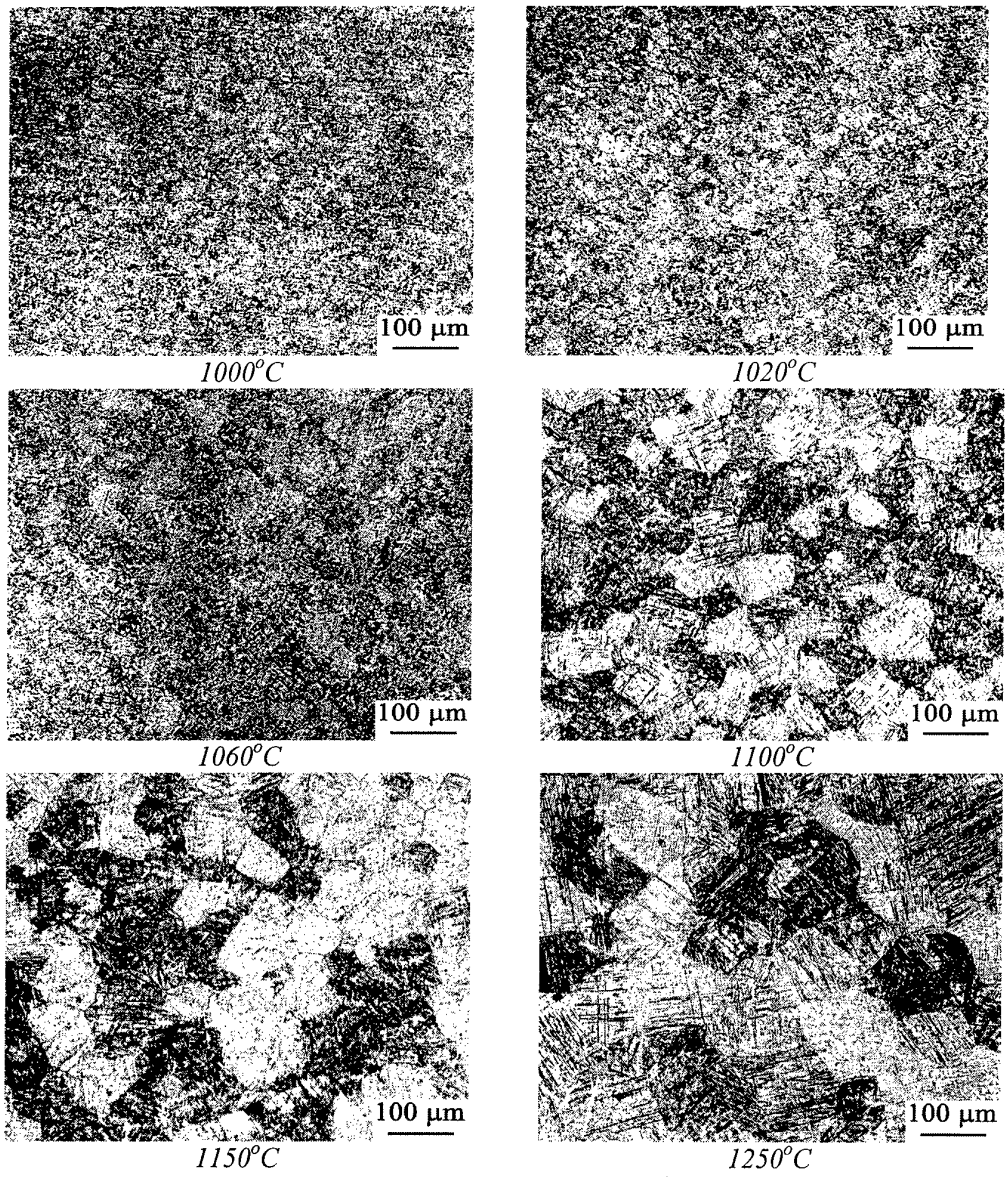

Figure 3.2. Grain growth in Ti-6Al-4V SM, at $\dot{T}$ =50 Ks^{-1}.

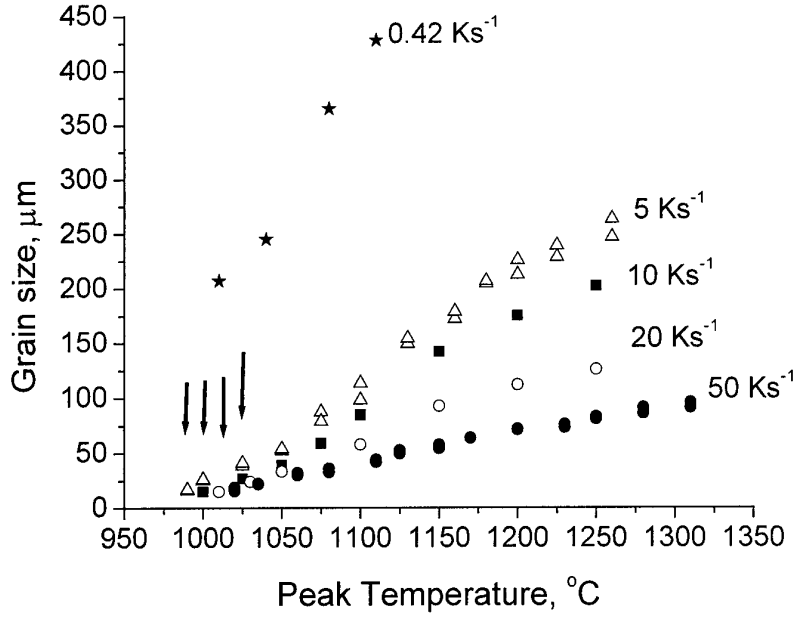

Figure 3.3. Beta-grain growth in PM at different heating rates. β - transus temperatures for each heating rate are shown by arrows.

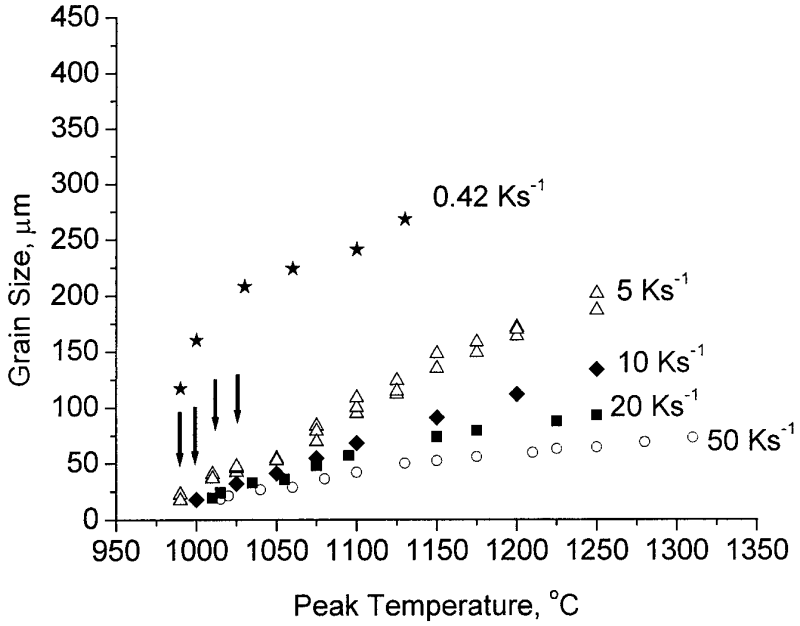

Figure 3.4. Beta-grain growth in SM at different heating rates. β - transus temperatures for each heating rate are shown by arrows.

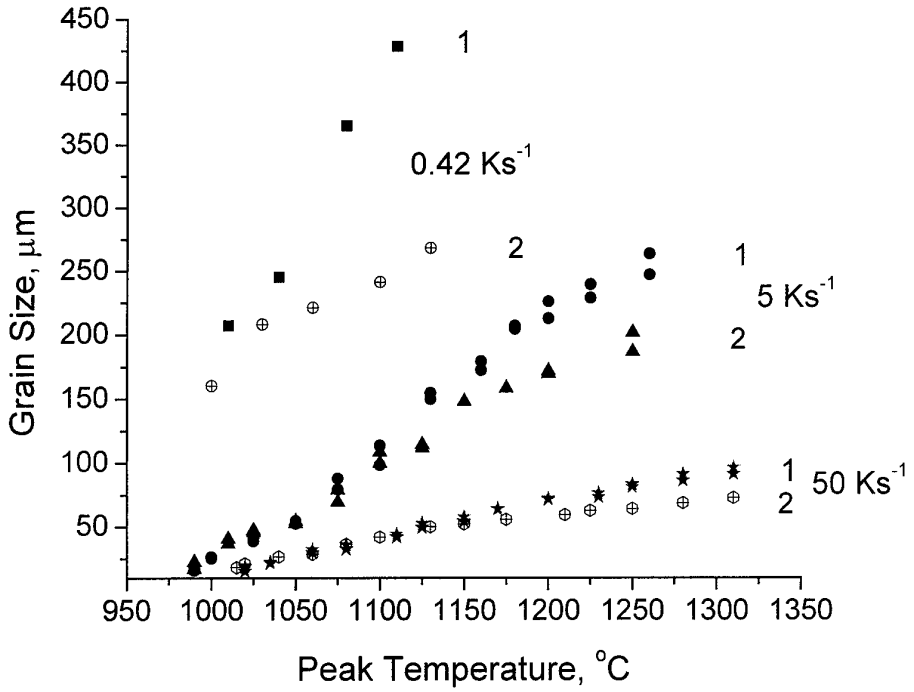

Figure 3.5. Comparison of beta-grain growth in (1) PM (2) SM.

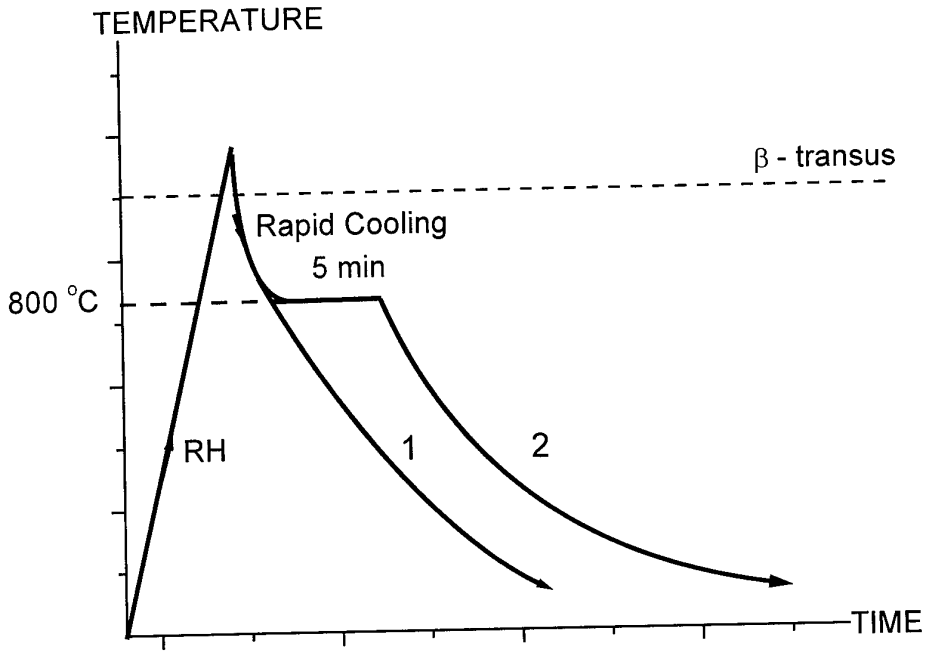

Figure 3.6. Scheme of cooling procedure of specimens intended for texture analysis.

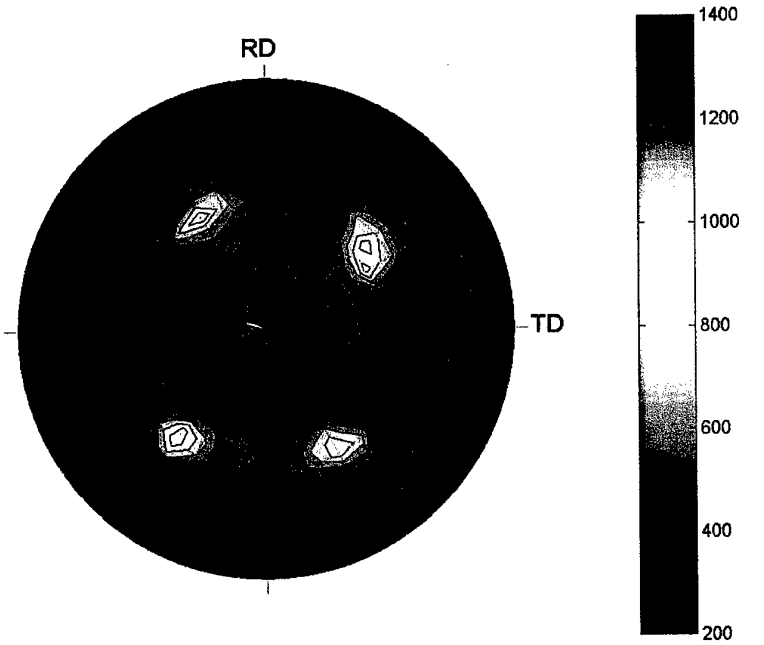
RD
TD
1400
1200
1000
800
600
400
200

1000°C

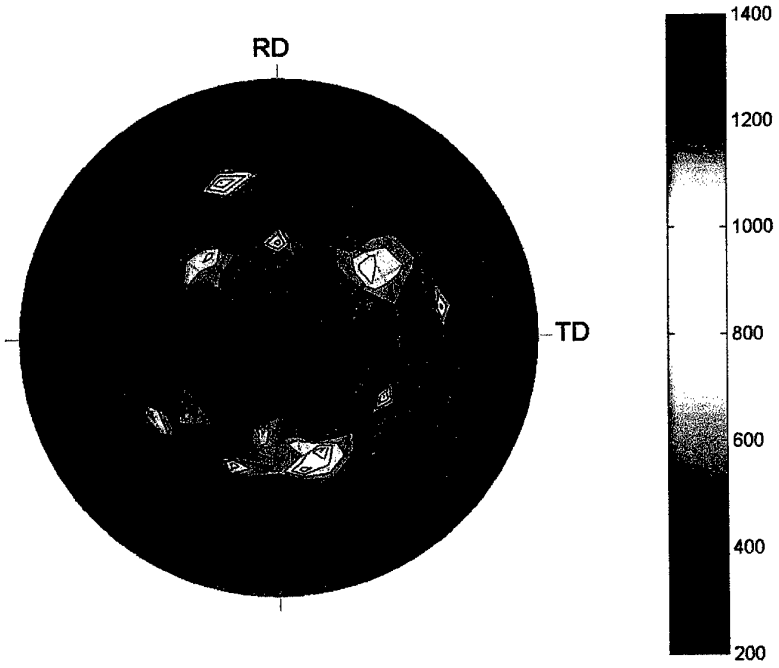
RD
TD
1400
1200
1000
800
600
400
200

1050°C

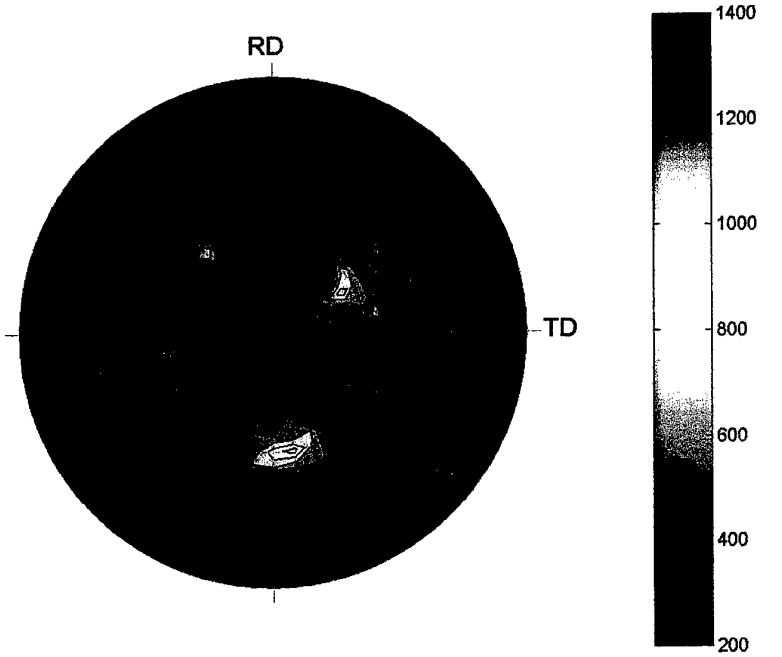
RD
TD
1400
1200
1000
800
600
400
200

1100°C

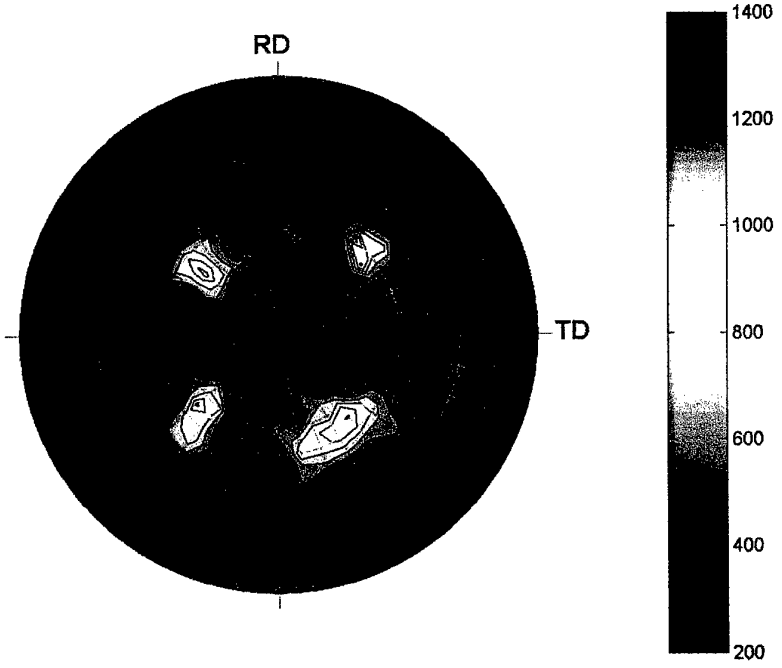
RD
TD
1400
1200
1000
800
600
400
200

1150°C

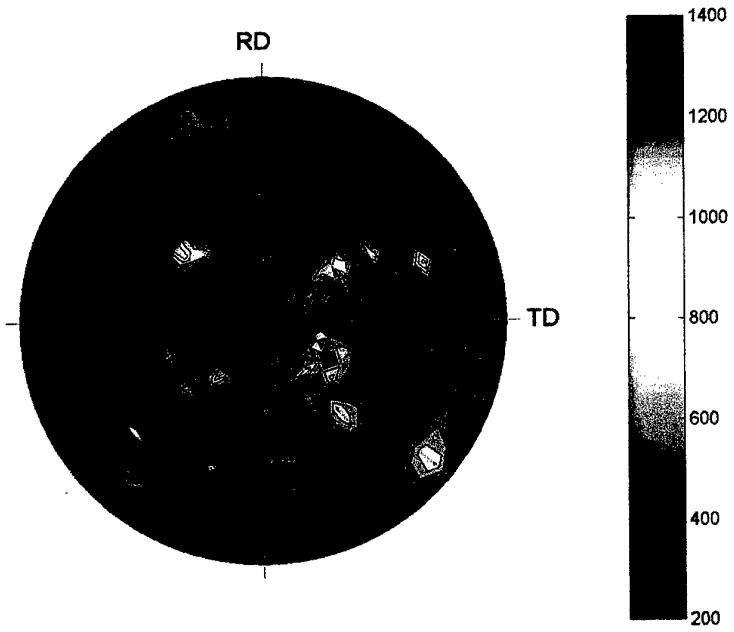

1200°C

Figure 3.7. (110) beta phase pole figures for SM, $\dot{T}$ =10 Ks^{-1}.

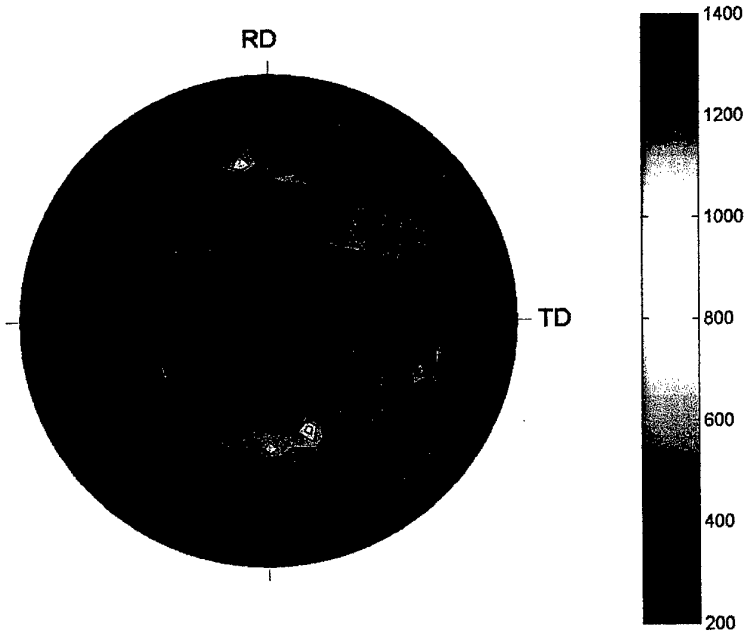

Figure 3.8 (110) beta phase pole figure of SM, T= 1180°C, $\dot{T}$ =50 Ks^{-1}.

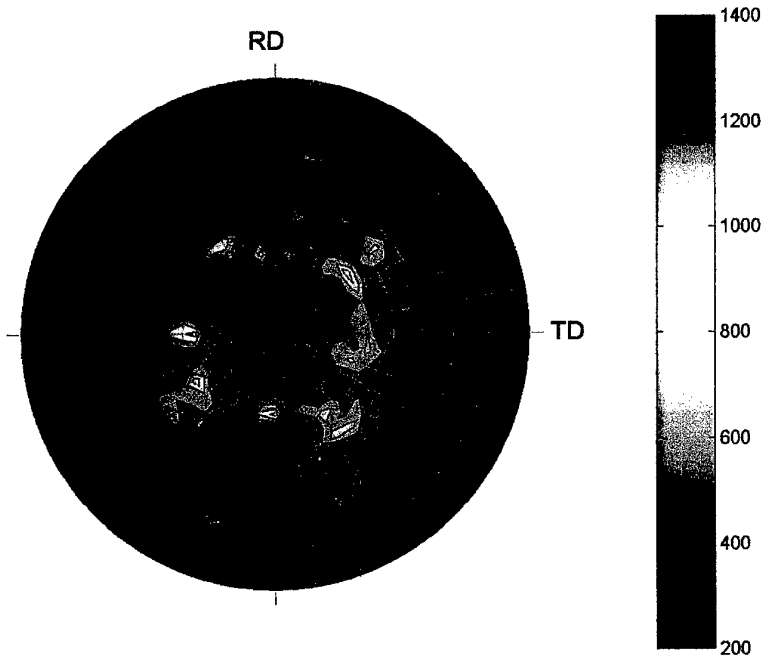

a)

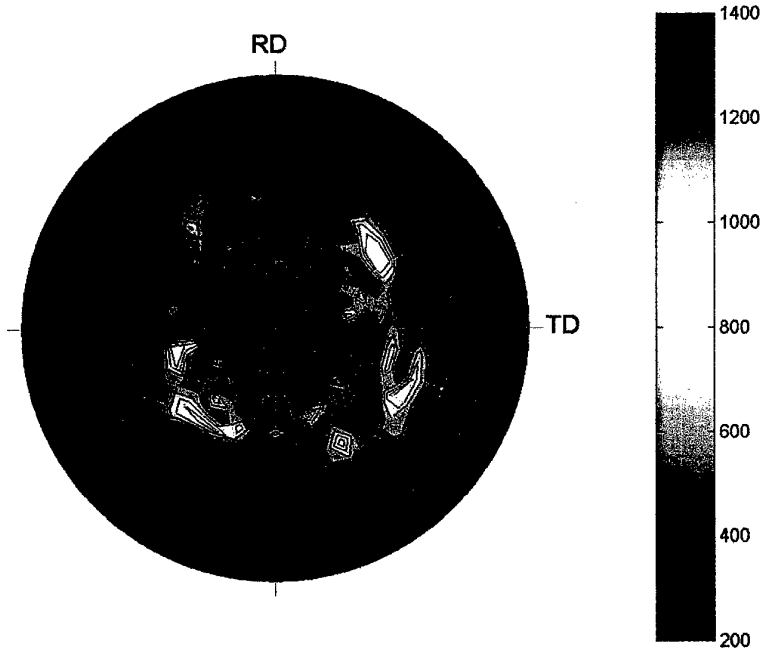

b)

Figure 3.9. (110) beta phase pole figure for PM heated to 1150°C: $\dot{T}$ = (a) 10 Ks^{-1}; (b) 50 Ks^{-1}

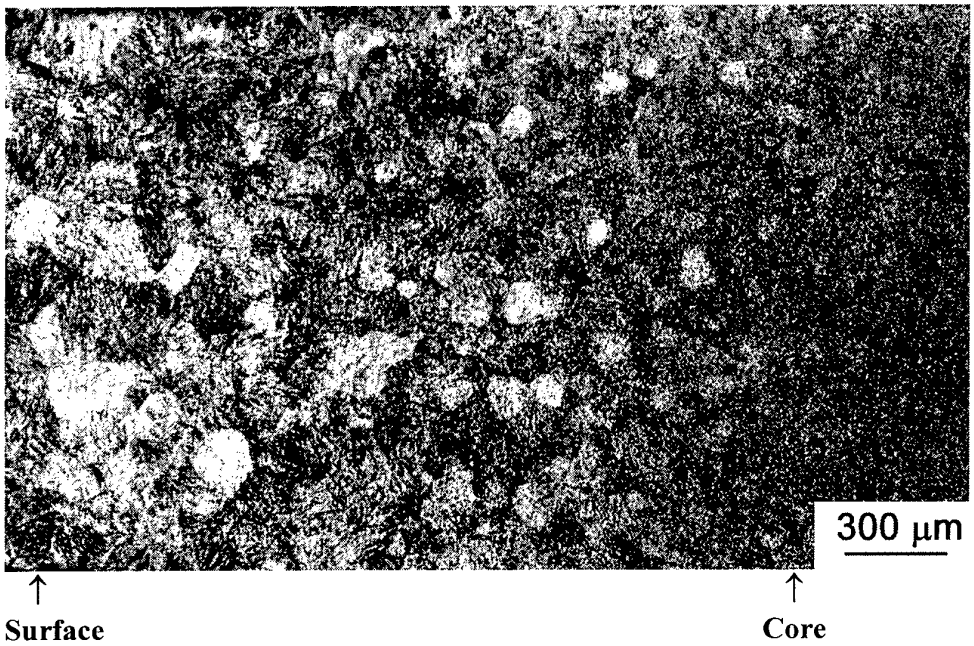

Figure 3.10. PM after induction heating to peak temperature (at the surface) 1250°C with heating rate 20 Ks^{-1} followed by rapid cooling.

4. Experiments on isothermal beta grain growth.

The aim of the experiments on isothermal beta grain growth was to check if an the assumption made in [2.1] that material coefficients Q and n are temperature independent above the beta transus, could be an acceptable approximation for the beta grain growth modeling at continues heating.

Isothermal annealings were performed in a vacuum furnace at temperatures of 1000, 1030, 1060, 1100, 1130, 1160, 1200, 1230, and 1260°C. At each temperature, specimens were exposed for various times, from 5 to 180 minutes. Unusually small temperature increment in isothermal experiments was aimed at most accurate determination of grain growth activation energy Q and grain growth exponent n in equation (1) within the given temperature range. After isothermal exposure specimens were cooled in furnace with an initial cooling rate not less than 50 Ks^{-1} using intensive water cooling of the furnace chamber. This allowed to prevent beta-grain microstructure reached at peak temperature from further growth upon cooling. Following the isothermal treatment, specimens were studied by means of quantitative metallography. The average grain sizes were determined by using the linear intersections method. Grains close to the surface were not taken into account. For both materials, standard deviation for average grain sizes was about 17-20% and confidence interval was ±5%.

Figure 4.1 presents typical microstructures of the SM and PM after some identical isothermal annealings. "Average beta grain size vs. annealing time" graphs comparing data for PM and SM materials at equivalent annealing parameters are shown in Figure 4.2. Figure 4.3 is another view of the same data, this time separately for PM and SM at different temperatures. In most cases experimental data are restricted by 1.0-1.2mm for PM and 0.3-0.4mm for SM, what is about one fifth of cross section smallest dimension, to be sure that edge effects are not important. Preliminary analysis of Figures 4.2 and 4.3 allows to conclude that, similar to the case of continues heating, PM exhibits much faster beta grain growth than that in the SM. Second obvious result well seen from Figures 4.2 and 4.3 is that experimental data for SM look like a result of discontinuous beta grain growth, having a significant zone of stagnation when average beta grain size is about 250-300 μm, contrary to PM, which exhibits rather typical isothermal behavior.

On Figures 4.4 and 4.5, ln(D)) vs. ln(t) graphs for both materials are present. According to (1), the slopes of these graphs should characterize the n value, however, it is evident from Figures 4.4 and 4.5 that n does not remain constant in investigated temperature range. Moreover, ln(D) vs. ln(t) graphs look quite different for SM and PM. Grain growth in PM can be characterized by certain n value for each annealing temperature, which, however, is temperature dependent (Figure 4.4). Sigmoidal type dependence n(**T**) was found for the PM (Figure 4.6) which allows to assume a slowering of grain growth at higher temperatures when grain size is big. For the SM, n(**T**) dependence is even more complicated. At lower annealing temperatures the slope of ln D vs ln t gives the averaged n value about 8.9, that means a very slow grain growth. At temperatures above 1100°C the grain growth rate increases with both

temperature and time. The stage of grain growth stagnation observed at these temperatures when average beta grain size is about 250-300μm, changes to a relatively fast growth at longer times. The higher the temperature, the shorter exposure is necessary for fast growth to start. Averaging data for 15 to 60 minutes time interval gives the n value of 3.9. With such n value, the activation energy Q for SM was estimated as 0=227kJ/mol from corresponding ln (D) vs. ln (1/**T**) graphs (Figure 4.7). Despite the ln(D) vs. ln (1/**T**) graphs for PM look like straight lines (Figure 4.8), however evaluation of activation energy Q in this case can not be done taking into account the sigmoidal n(**T**) dependence.

It could be concluded from the above results that the description of beta grain growth kinetics in the terms of grain growth exponent and activation energy independent of temperature for both investigated materials seems to be impossible.

References.

2.1. Semiatin S.L., Fagin P.N., Glavicic M.G, Sukonnik I.M., and O.M. Ivasishin. Influence of Texture on Beta Grain Growth During Continuous Annealing of Ti-6A1-4V. Mat. Sci. And Eng. , V. A299, 2001, pp. 225-234.

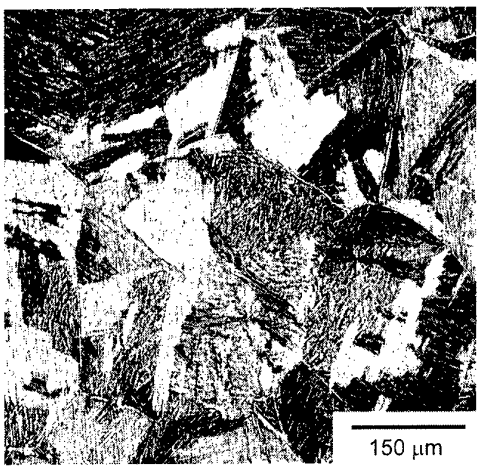

SM, 1100°C, 5 min

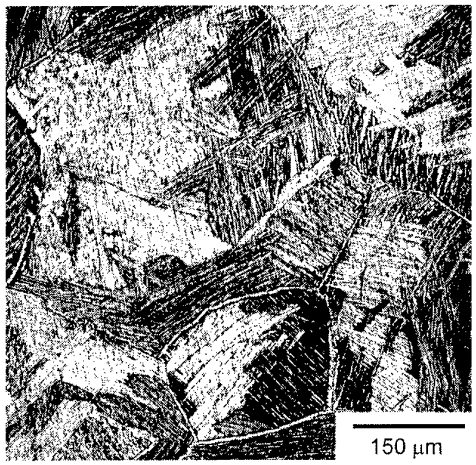

PM, 1100°C, 5 min

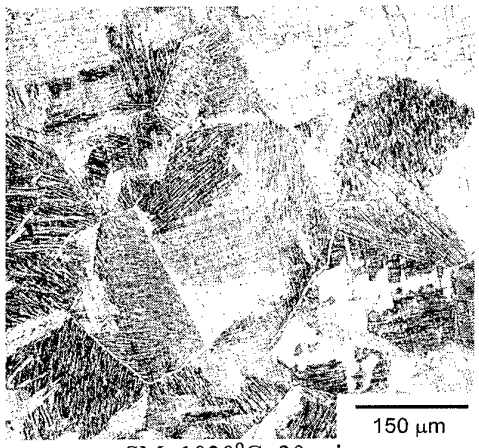

SM, 1030°C, 30 min

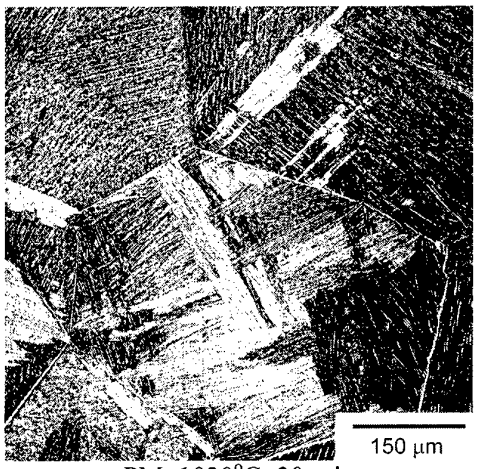

PM, 1030°C, 30 min

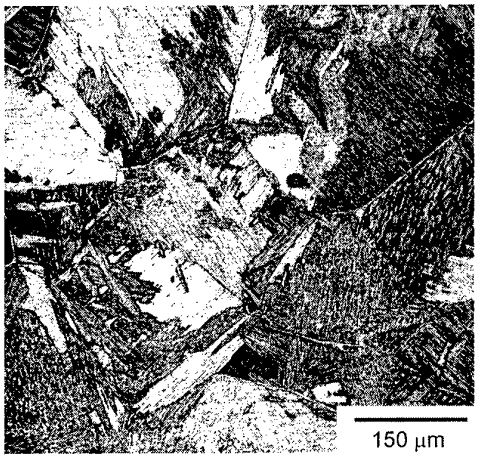

SM, 1100°C, 15 min

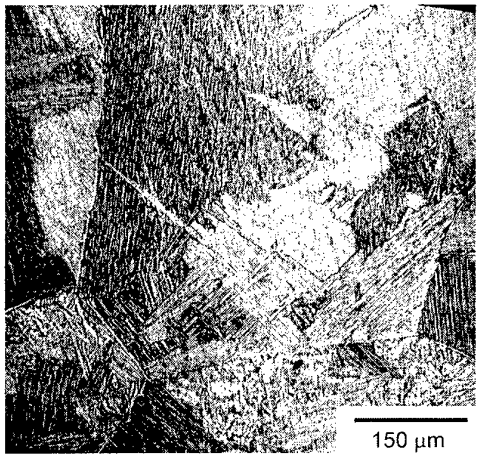

PM, 1100°C, 15 min

Figure 4.1. Microstructures of PM and SM after isothermal annealing.

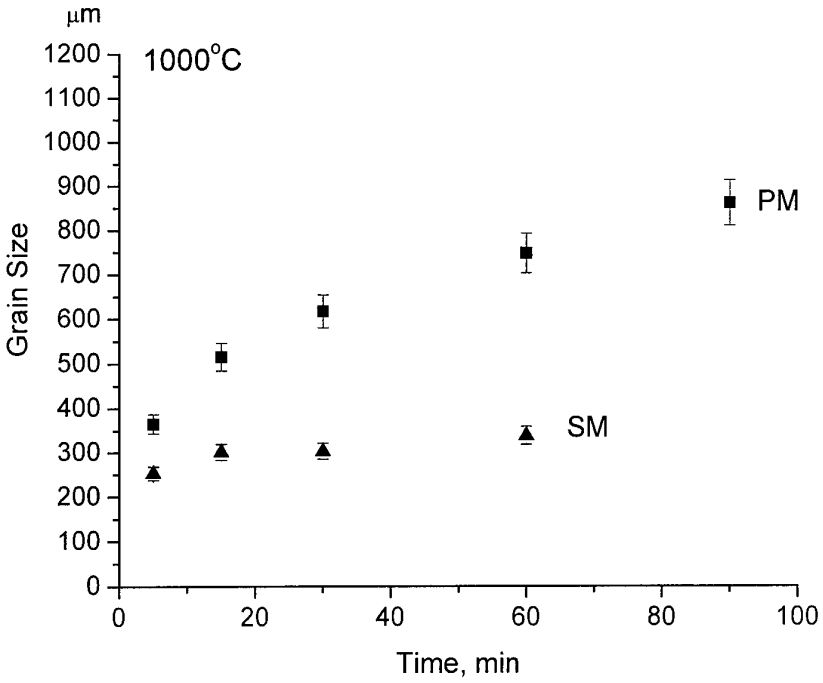
μm
1000°C
Grain Size
PM
SM
Time, min
0
100
200
300
400
500
600
700
800
900
1000
1100
1200
0
20
40
60
80
100

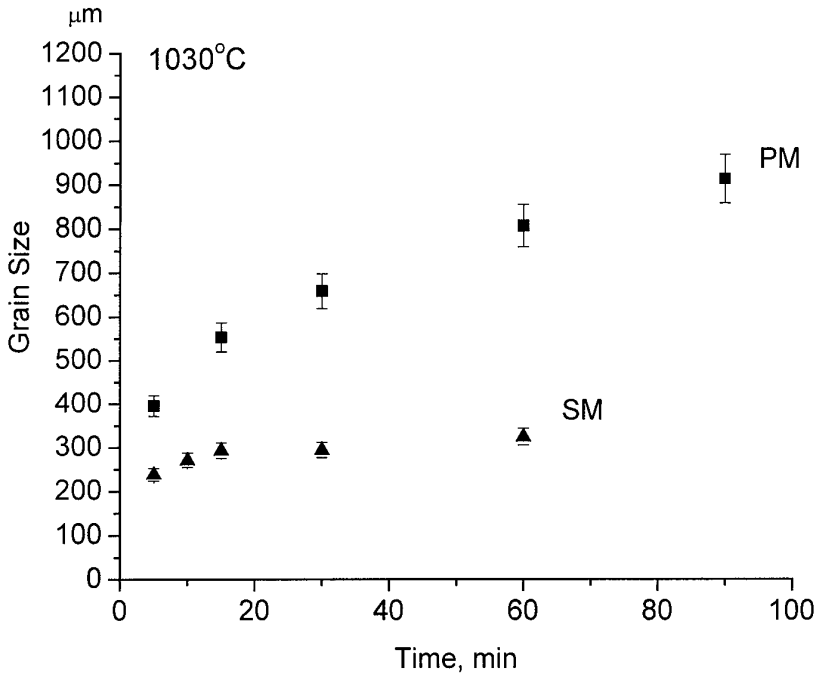
μm
1030°C
Grain Size
PM
SM
Time, min
0
100
200
300
400
500
600
700
800
900
1000
1100
1200
0
20
40
60
80
100

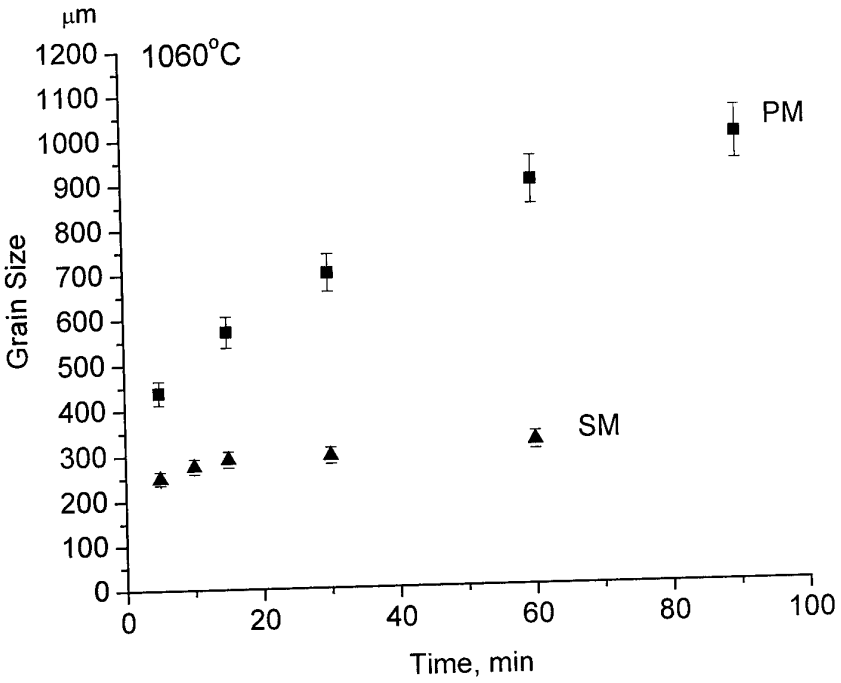
μm
1060°C
PM
SM
Grain Size
Time, min
0
100
200
300
400
500
600
700
800
900
1000
1100
1200
0
20
40
60
80
100

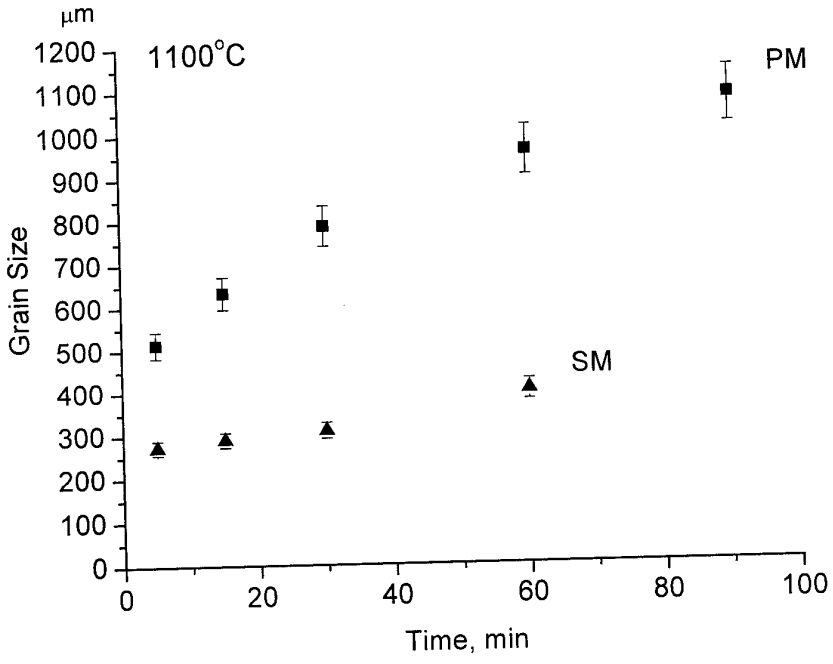
μm
1100°C
PM
SM
Grain Size
Time, min
0
100
200
300
400
500
600
700
800
900
1000
1100
1200
0
20
40
60
80
100

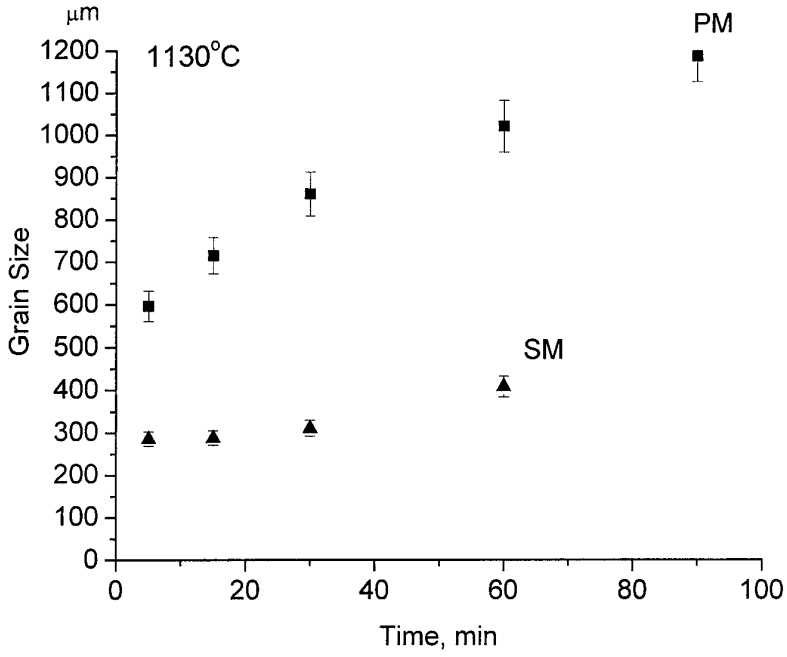
μm
1130°C
PM
SM
Grain Size
Time, min
0
100
200
300
400
500
600
700
800
900
1000
1100
1200
0
20
40
60
80
100

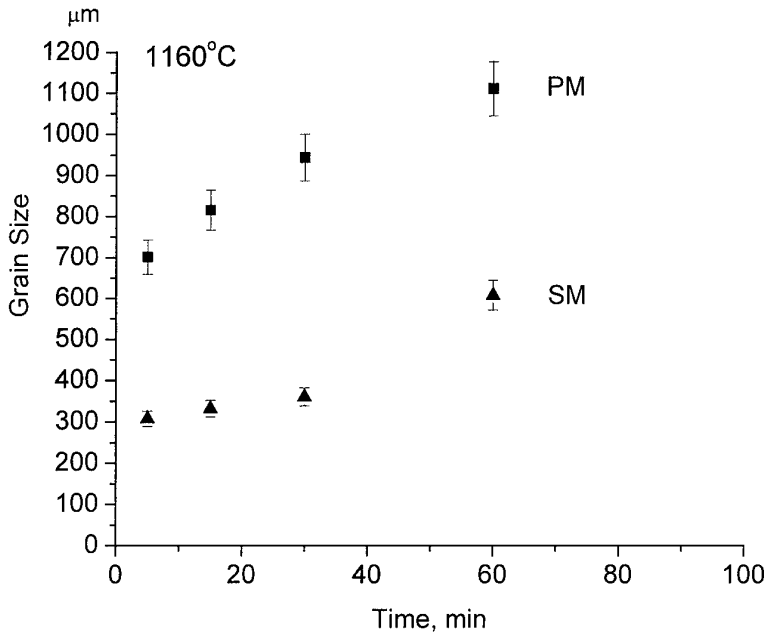
μm
1160°C
PM
SM
Grain Size
Time, min
0
100
200
300
400
500
600
700
800
900
1000
1100
1200
0
20
40
60
80
100

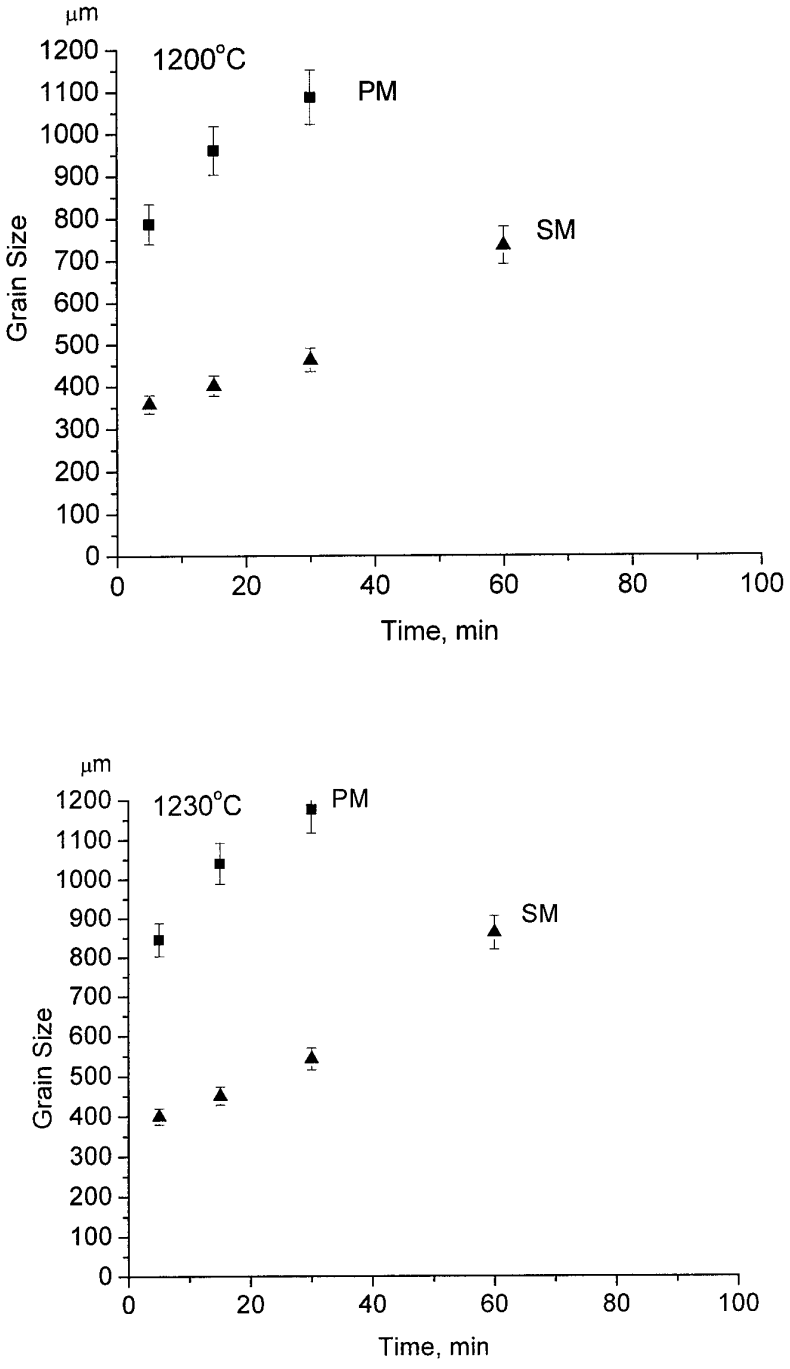

Figure 4.2. Average grain size vs. annealing time for PM (■) and SM (▲).

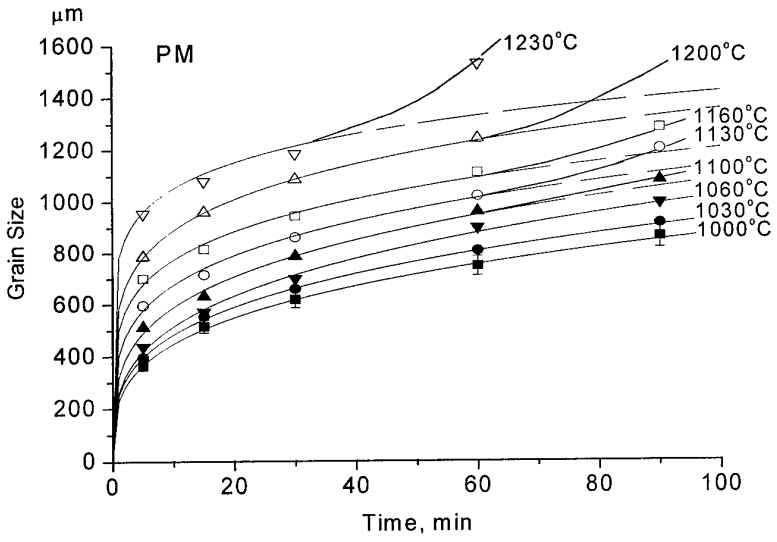

a)

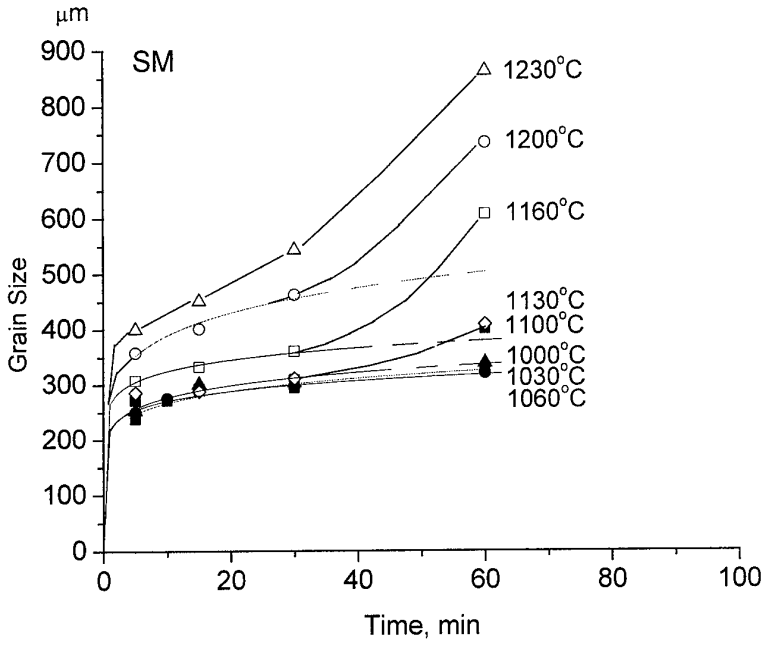

b)

Figure 4.3. Average beta grain sizes vs. annealing time for (a) PM and (b) SM.

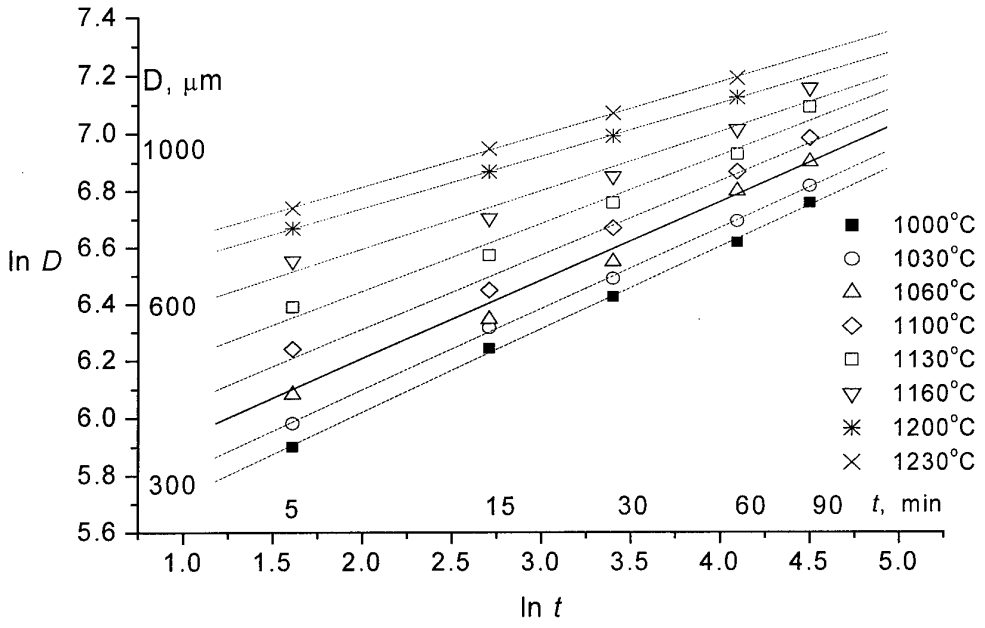

Figure 4.4. Ln D on ln t dependencies for PM at various temperatures.

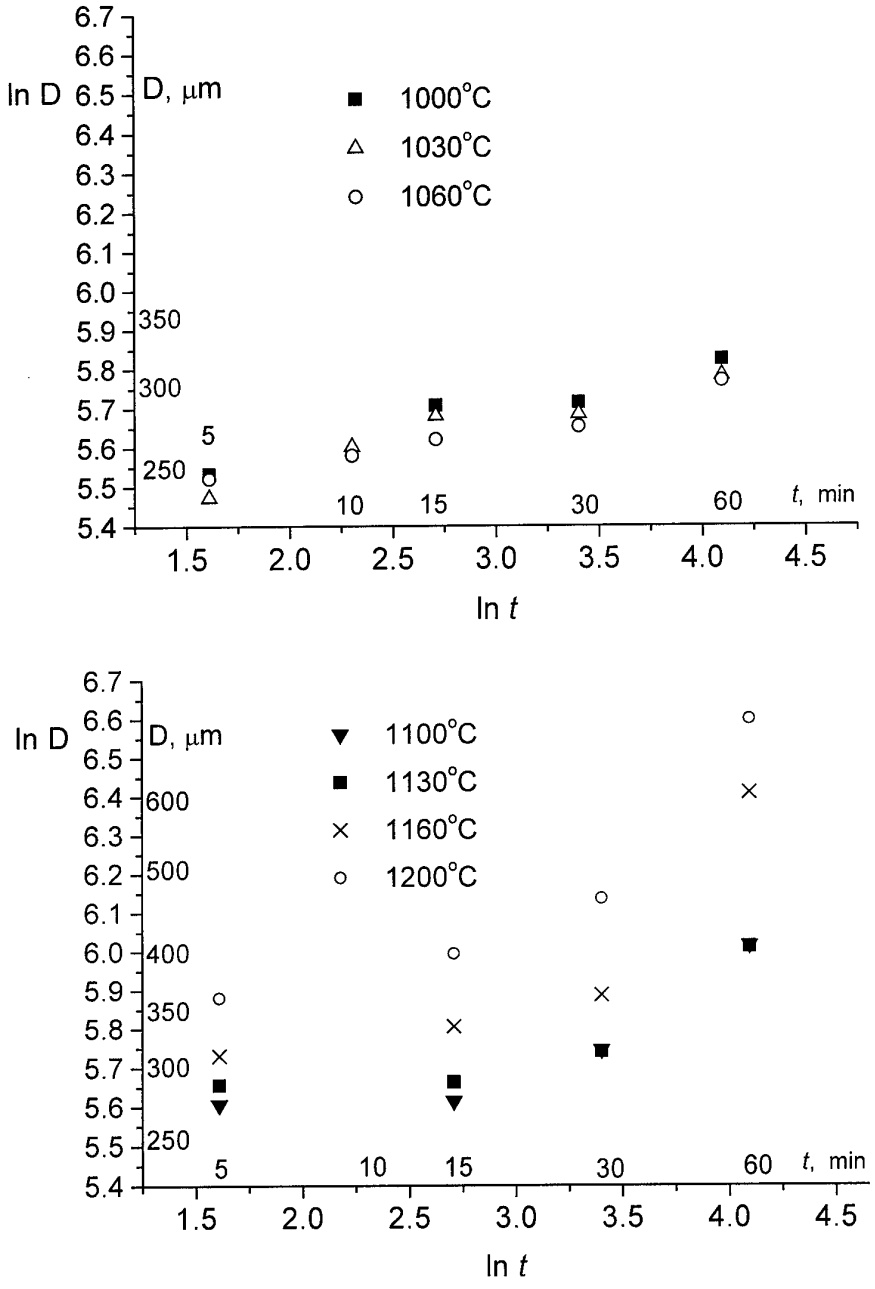

Figure. 4.5. Ln D on ln t Dependencies for SM at various temperatures.

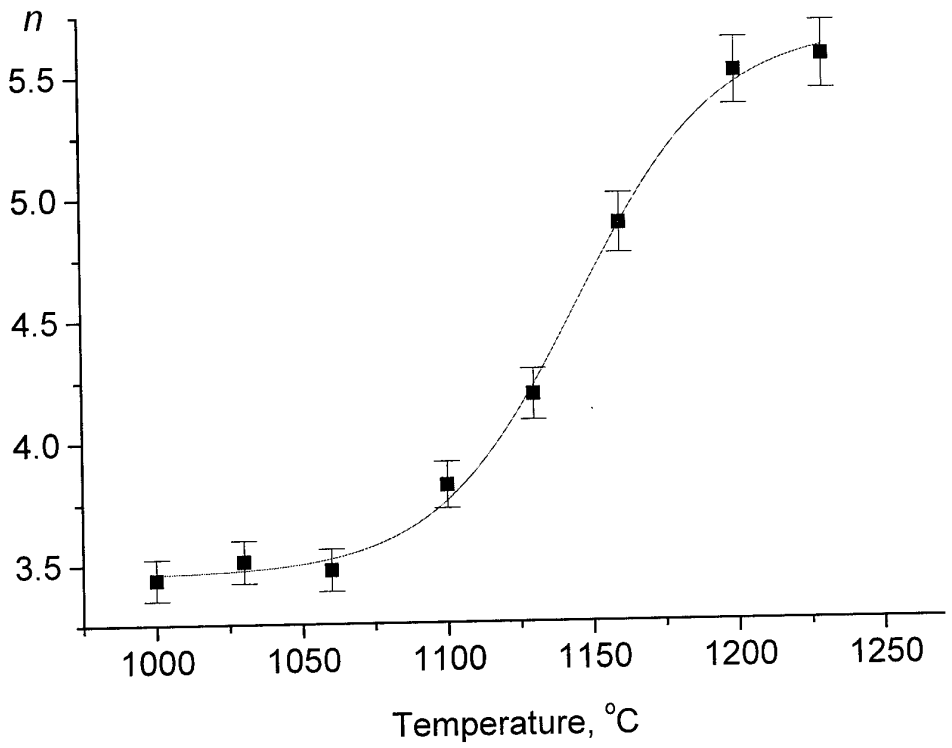

Figure 4.6. Temperature dependence of grain growth exponent n for PM.

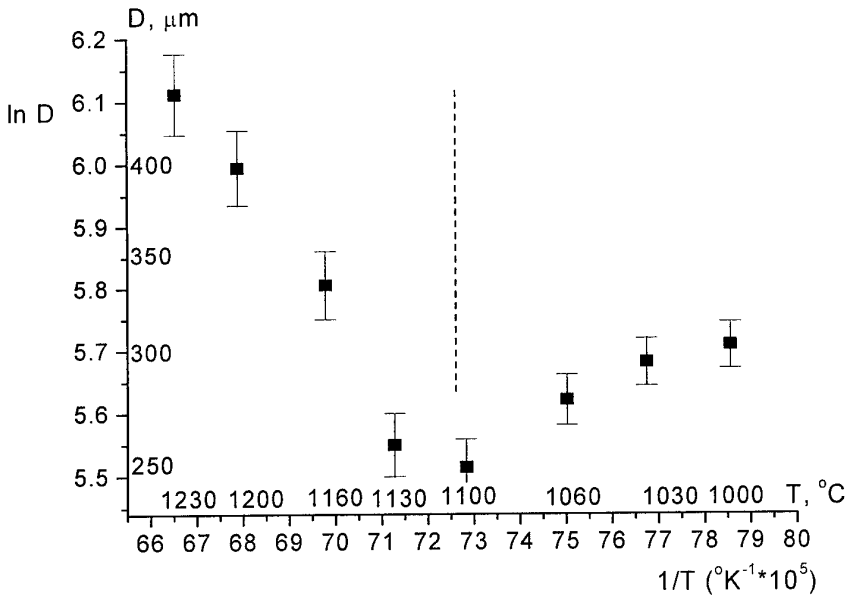

a)

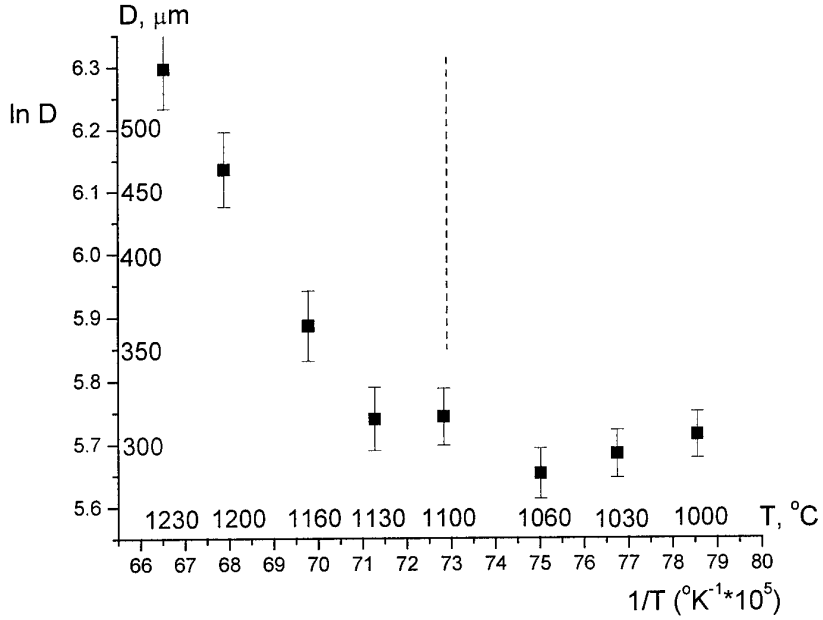

b)

Figure 4.7. Ln*D* vs. ln (1/**T**) graphs for SM (a) t=15min and (b) t=30min.

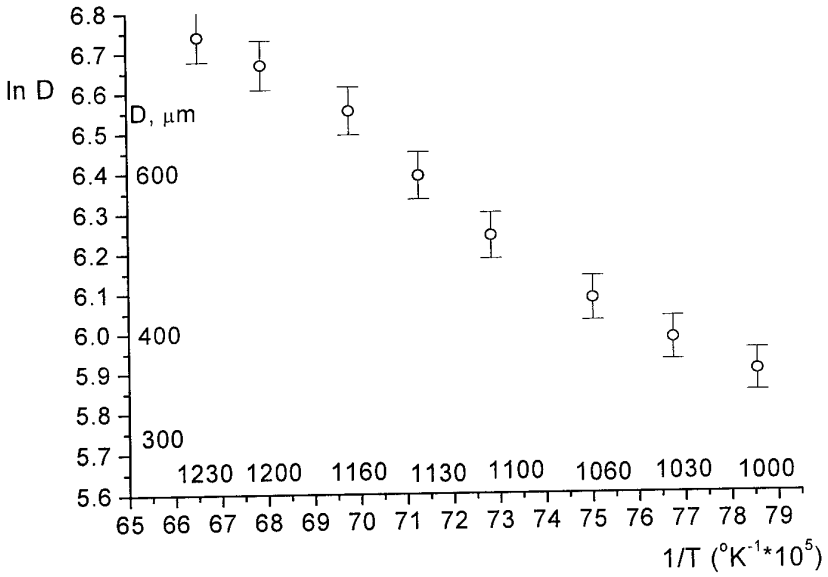

a)

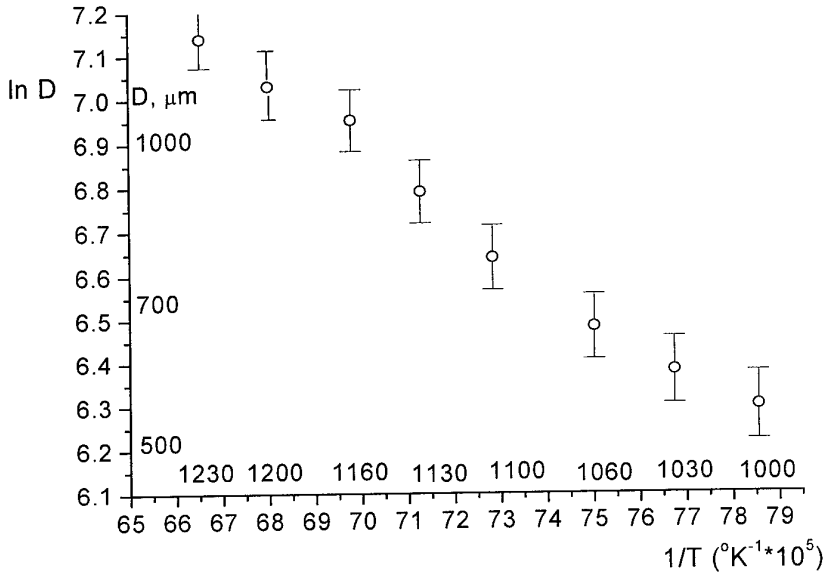

b)

Figure 4.8. Ln*D* vs. ln (1/**T**) graphs for PM (a) t=15min and (b) t=30min.

5. Discussion.

Experimental data on beta grain growth at both continuous and isothermal treatments are consolidated on Figure 5.1. As it was concluded in section 4 from the isothermal grain growth results, material coefficients (grain growth exponent n and activation energy Q) are not constant in beta phase field. The most adequate explanation of this is that texture affects integral grain boundary mobility. In turn, this implies that approach developed in [5.1] for grain growth modeling on continuous heating seems to do not work in textured titanium alloys. For instance, comparison of experimental and calculated in accordance to [5.1] data shows an essential discrepancy at high temperatures, which is more pronounced in SM but well resolved in PM as well (Figure 5.2).

As can be seen from experimental data presented in sections 3 and 4 beta-grain growth kinetics are discontinuous in sense that stages of relatively fast (normal) grain growth and growth slowering are alternate. At isothermal annealing, this phenomenon is well observed in SM: at all temperatures after initial period of fast growth of beta grains during first 5 min to about 250 μm, further growth is very slow, if any (see Figure 4.3) until the second stage of fast growth begins. Time interval of slow growth is, certainly, shorter at higher temperatures; the temperature defines as well the grain size achieved by the end of one-hour exposure: 400, 600, 750, and 900 μm at 1130°C, 1160°C, 1200°C, and 1230°C respectively. In PM periodical rate of grain growth is not so evident at exposures employed; the increase in grain growth rate is clearly observed only at high temperatures. Just at these temperatures starting n value was about 5.6. (see Figure 4.6) that corresponds to a relatively slow growth. It should be noted that discontinuous grain growth kinetics was observed earlier in IMI685 and IMI318 (Ti-6Al-4V) [5.2] (Figure 5.3). Stephen Fox assumed a material texture to be the most possible reason for a very slow grain growth, which speeded up after long exposure.

Employing of very rapid, continuous heating (50 Ks^{-1}) allows to observe the very first slowering of the grain growth when grain size gets 50-70 μm level (see Figure 5.2). On the other edge, isothermal annealing exhibits second slowering at above 200 μm level. To reach this second slowering while heating with the rate of 50 Ks^{-1} is technically impossible; temperatures in excess of 1500°C would be necessary for this. Lower continuous heating rates, 5 and 0.42 Ks^{-1} give a unique possibility to realize an intermediate situation in sense that grain structure evolution during continuous heating looks very much like that at isothermal annealing. However, with lower heating rates, a resolution of first slowering is not so evident (5 Ks^{-1}) as at 50 Ks^{-1}, or impossible at all (0.42 ks^{-1}).

Hence, we can summarize main features of grain growth kinetics at continuous heating by schematic temperature dependencies of beta grain size at three various heating rates $\dot{\mathbf{T}}_1 < \dot{\mathbf{T}}_2 < \dot{\mathbf{T}}_3$ with two levels of grain growth slowering, on which

experimental data for SM are imposed (Figure 5.4). Discontinuous character of grain growth in PM is less pronounced than in SM, i.e. similar chart for PM would differ only by lesser deviation from normal grain growth behavior.

Texture effects seem to be the only possible explanation of the above results. It was shown analytically [5.3] that texture evolution during annealing can drastically change normal grain growth kinetics. Numerical modeling was performed in [5.3] for the case of two texture components A (main component) and B taken in 10/1 fraction volumes and in assumption that $M_{BA}=M_{AB}=5M_{AA}=5M_{BB}$ (Figure 5.5). Due to their smaller number, the B grains have a much higher probability to be surrounded by A than B grains and thus by high mobility B-A boundaries. Hence, the smaller ones of the B grains will be rapidly consumed by the larder A grains, but the larger B grains will be able to grow rapidly. Since the A grains are in contact preferably with A grains, they will be surrounded mainly by low mobility A-A boundaries, so that most of A grains participate only little in the grain growth process. After the B grains have taken over a larger part of the volume, the growth rate of the B grains decreases, since then they are now surrounded also by B grain. When finally A becomes the minority component, the growth rate of A grain supercedes that of B grains. This explains the behavior of the overall average grain size. Since average grain size is always close to the partial average radius of the majority component, it stays initially close to the average radius of the A grains and then increases steeply to the values close to the average radius of the B grains. This looks like an accelerated grain growth after initial stagnation and yields the impression of a sort of discontinuous growth. Performed for the longer times, modeling yields to the cyclic interchanges of volume fractions of A and B components (Figure 5.6.) and of grain growth rate respectively. The cyclic behavior of some metals was confirmed experimentally in [5.4]. In literature, several results are documented which can be considered as a texture evolution in Ti-6Al-4V like that presented on Figure 5.5. In [5.5], the interchange of volume fraction of two components, specifically {001}<110> and $\{112\}<1\bar{1}0>$ in beta phase field was observed. Recently, it has been shown in [5.6] that the texture of high-temperature beta phase after isothermal heat treatment slightly above beta-transus is (*a*) very sharp and (*b*) of the same type as initial texture. Although the grain size of the beta phase is not reported in [5.6], it can be supposed from the present study to be not less than 250-300 μm. This may indicate that material has already come through randomizing of texture and developed a "secondary" texture in the beta phase.

Some evidence of that during continuous heating, texture of titanium alloys come through a cyclic evolution, which can be a reason of alternating stages of fast and slow grain growth was received in this study. A very fast randomizing of texture at low beta temperatures yields an equivalent kinetics for SM and PM above beta transus. Then a gradual formation of secondary texture, more evident in SM because SM has more textured initial microstructure, deviates the growth kinetics from normal

exponential law (slow growth). At higher temperature the texture will again come through a randomized textural condition, yielding the fast grain growth again, and so on. Temperature during continuous heating and time during isothermal heating are, to some extent, equivalent in a sense that they both are able to cause such periodical changes. Different materials have their own texture evolution therefore, their temperature dependencies of grain size should be always different.

References:

5.1. Semiatin S.L., Fagin P.N., Glavicic M.G, Sukonnik I.M., and O.M. Ivasishin. Influence of Texture on Beta Grain Growth During Continuous Annealing of Ti-6Al-4V. Mat. Sci. and Eng., V. A299, 2001, pp. 225-234.

5.2. Fox S.P. A Study of Grain Growth Behavior in Titanium Alloys. Proc. of Titanium'92, Science and Technology, ed. Froes F.H. and Caplan I.L. 1992, pp. 769-776.

5.3. Eichelkraut H., Abbruzzese G. and Luke K., A Theory of Texture Controlled Grain Growth-II. Numerical and Analytical Treatment of Grain Growth in the Presence of Two Texture Components. Acta metall., v. 36, 1988, pp. 55-68.

5.4. Grewen J. and Huber J. Recrystallization of Metallic Materials. ed. by Haessner, Riederer Verlag, Stuttgart (1978). p. 111.

5.5. Divinski S.V., Dnieprienko V.N and Ivasishin O.M., Effect of phase transformation on texture formation in Ti-base alloys, Mat. Sci. and Eng., v. A243, 1998, pp. 201-205.

5.6. Gey N., Humbert M. and Moustahfid H., Study of the alpha-beta phase transformation of a Ti-6Al-4V sheet by means of texture change, Scripta Mat., v. 42, 2000, pp. 525-530.

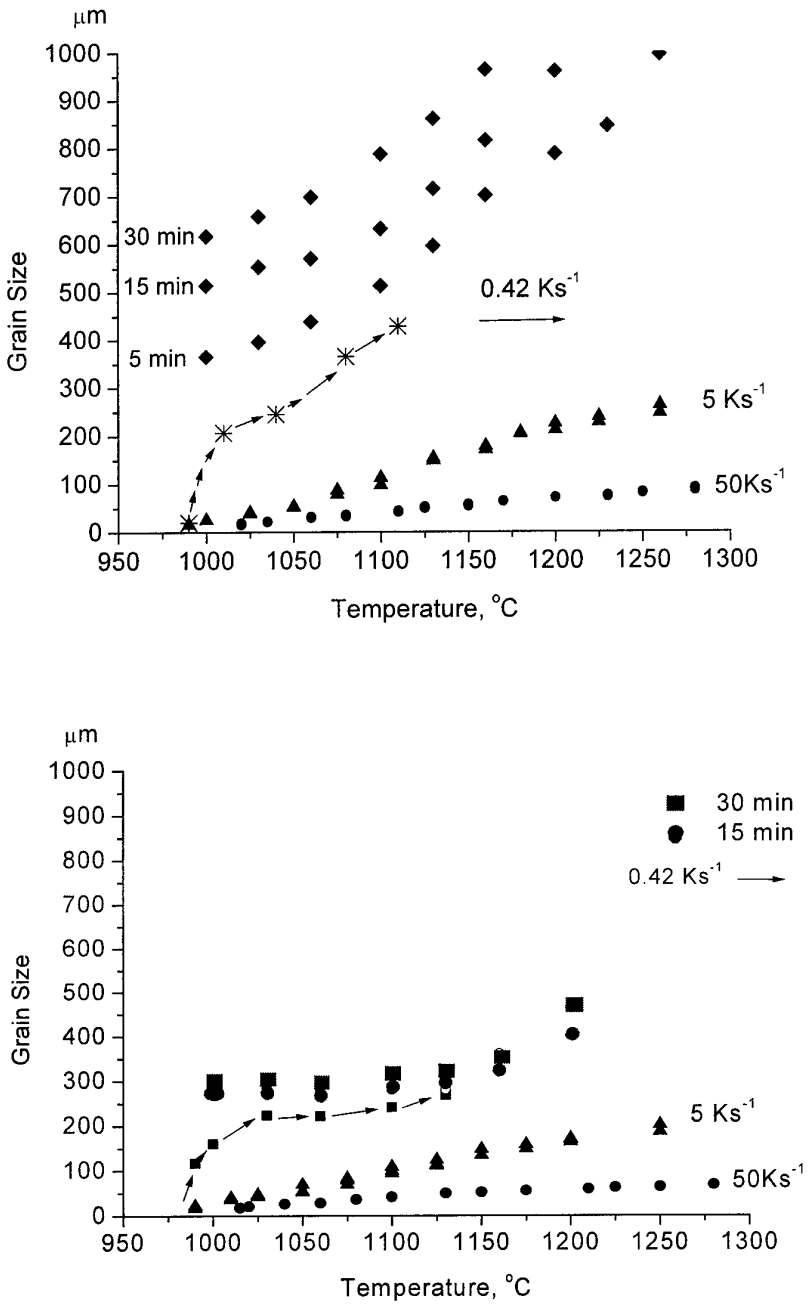

Figure 5.1. Consolidated temperature dependencies of beta-grain size for (*a*) PM and (*b*) SM.

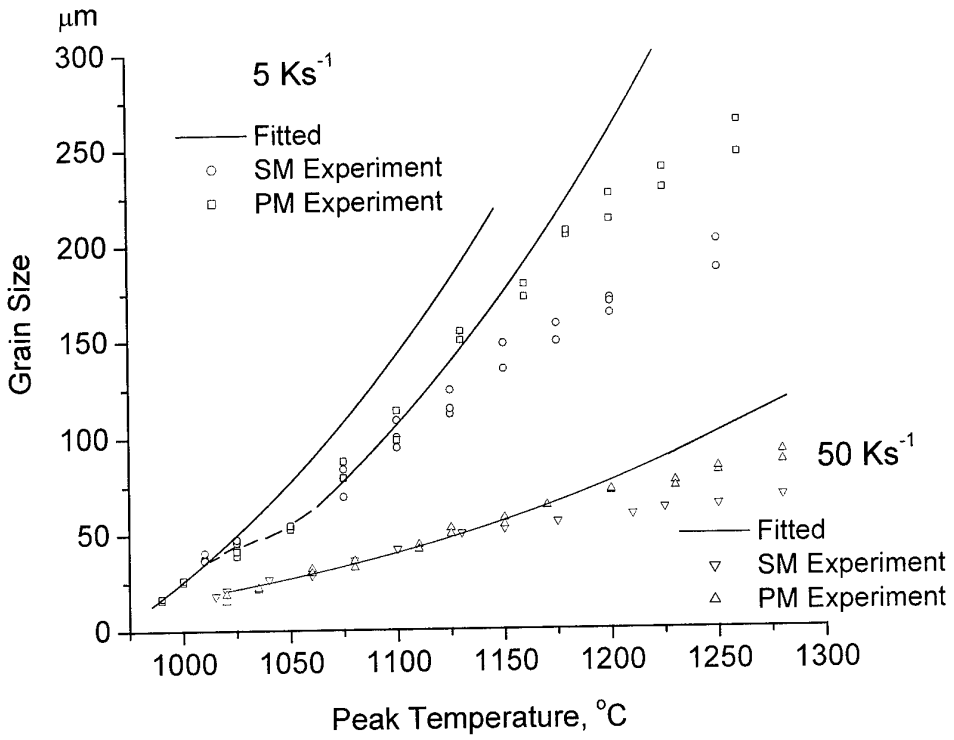

Figure 5.2. Fitting the beta grain growth model predictions to the experimental data.

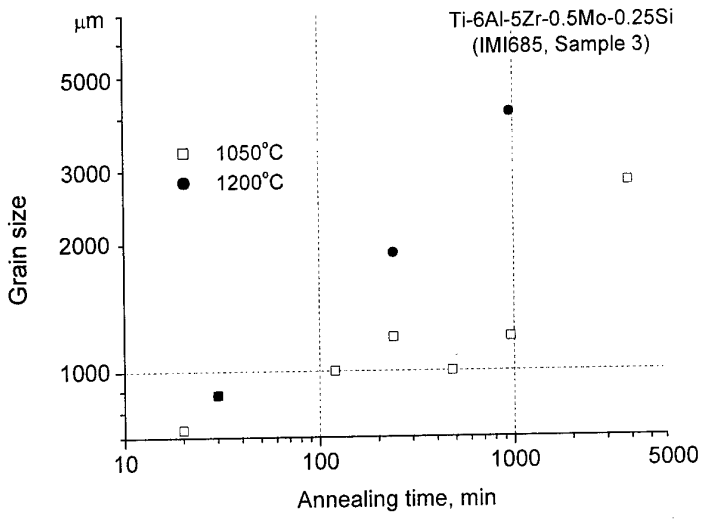

a)

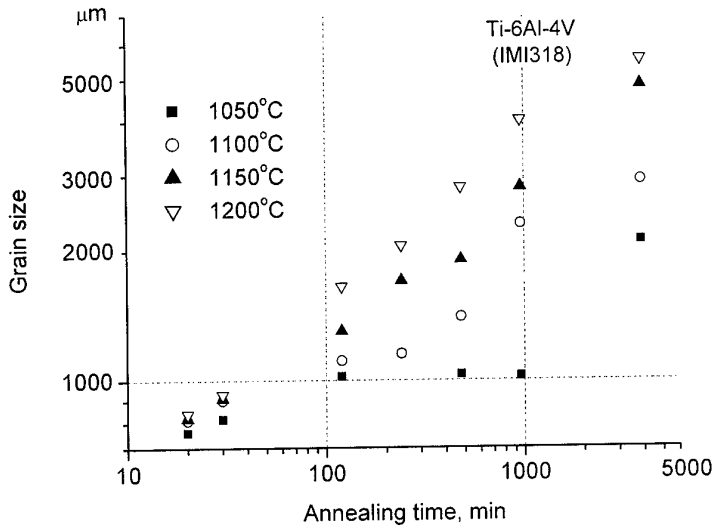

b)

Figure 5.3. Discontinuous grain growth in IMI685 (*a*) and IMI318 (*b*) alloys at isothermal annealing [5.2].

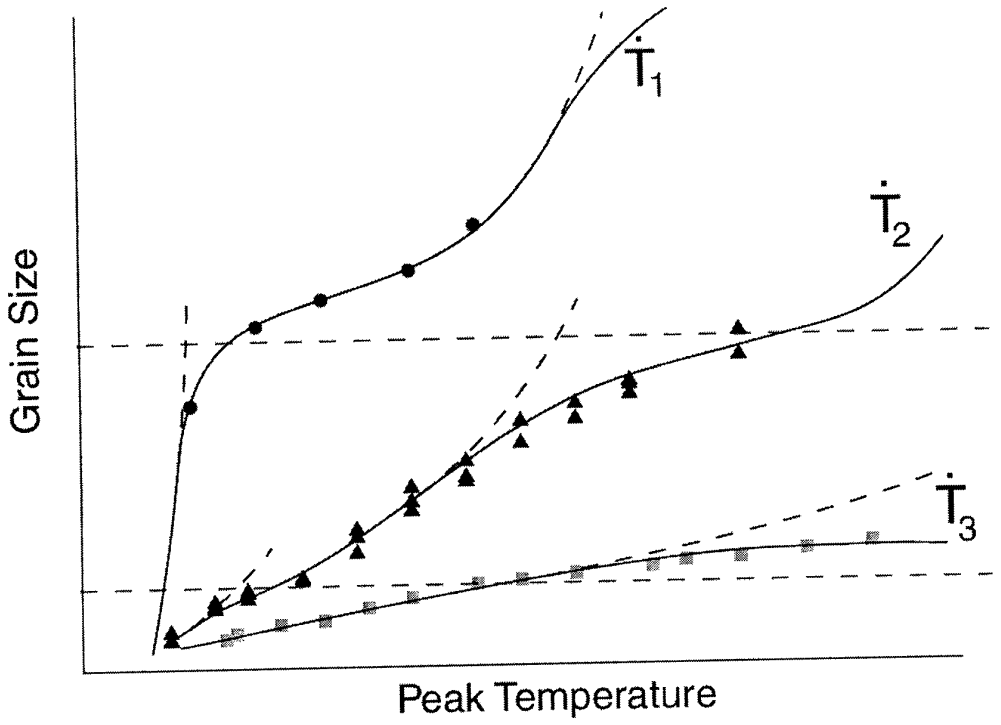

Figure 5.4. Schematic temperature dependencies of beta grain size at three heating rates $\dot{T}_1 < \dot{T}_2 < \dot{T}_3$ with two levels of grain growth slowering. Experimental data for (•) 0.42 Ks^{-1}, (▲) 5 Ks-1, and (■) 50 Ks-1 are plotted.

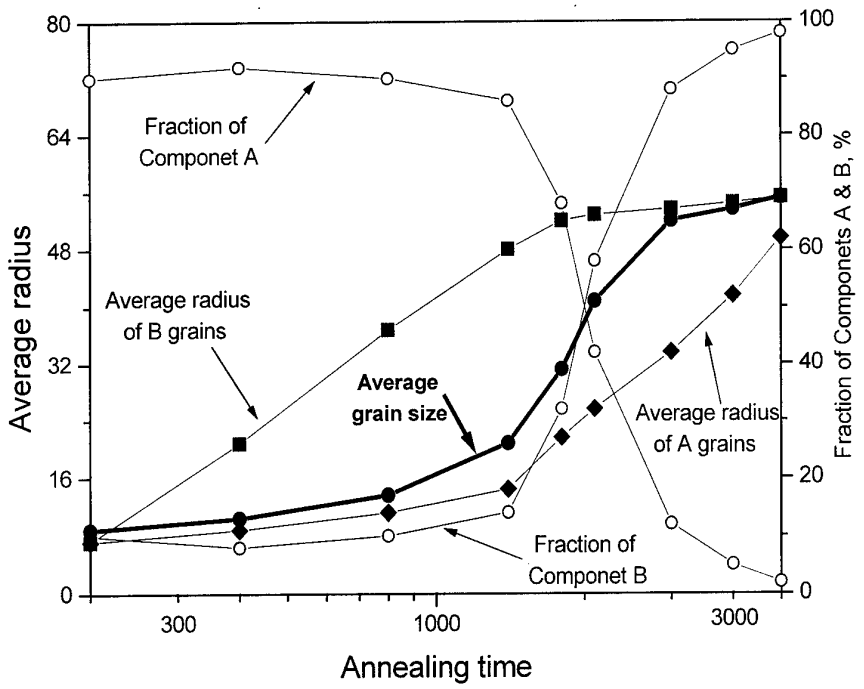

Figure 5.5. Modeling of texture development and grain growth at annealing in materials with two component texture [5.4].

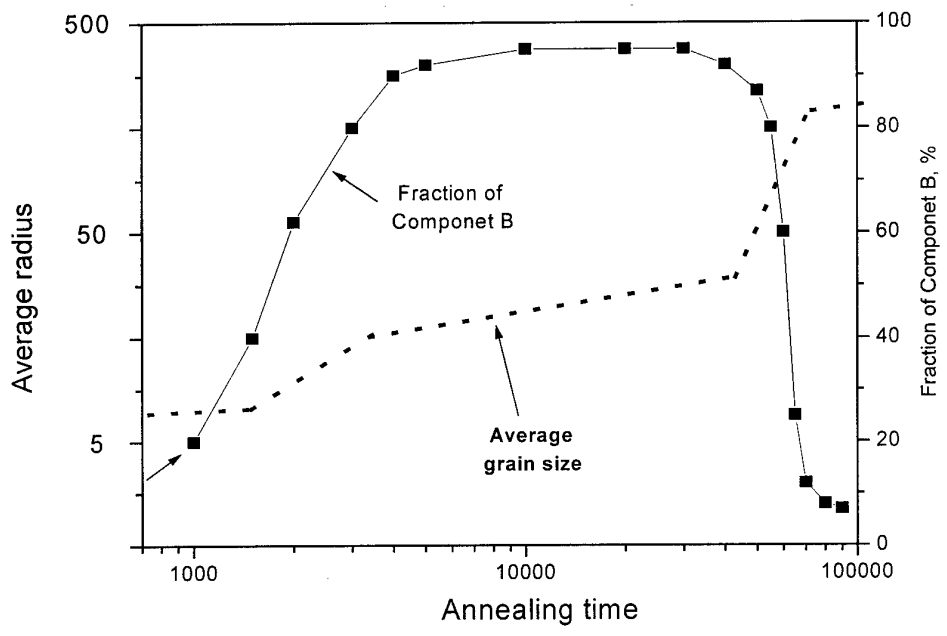

Figure 5.6. Modeling of texture development and grain growth during long time annealing.

6. Grain growth modeling (computer simulations).

Additionally to the project working plan, a development of 3D model of texture controlled grain growth using Monte-Carlo (MC) procedure was started. The aim of computer simulations was to model grain growth in b.c.c. materials and simultaneously, to control the textural state of the modeling space. The overview of up to date theoretical efforts devoted to this problem has shown that in most recent computer simulations of normal grain growth in two- and three-dimensional modeling space [6.1, 6.2] crystallographic orientation of grains was not taken into account. An original approach that allows to consider the effect of texture on grain growth kinetics, has been proposed in [6.3]. In the model [6.3] which is based on the Monte-Carlo (MC) technique the microstructure is mapped onto a discrete *two-dimensional* lattice. Each lattice site is assigned a number, between 1 and L, which indicates the local crystallographic orientation. The initial distribution of orientations is chosen at random and the system evolves so as to reduce the number of nearest neighbor pairs of unlike crystallographic orientation. Model volume does not contain grain boundaries, the grain boundary position is associated with the space between two sites having unlike orientations. The grain boundary energy is specified by defining an interaction between nearest neighbor lattice sites. The Hamiltonian describing this interaction is:

$$H = -J(\delta_{S_i S_j} - 1) \tag{8}$$

where S_i is one of the L orientations on site i ($1 \leq S_i \leq L$) and δ_{hl} is the Kronecher delta. The sum is taken over all nearest neighbor sites. Thus, nearest neighbor pairs contribute J to the system energy when they are of unlike orientation and zero otherwise.

The kinetics of boundary motion are simulated by the MC technique: a lattice site is selected at random, and a new trial orientation is also chosen at random from one of the other (L–1) possible orientations. The transition probability, W, is then given by:

$$W = \begin{cases} \exp(-\Delta G / k_b \mathbf{T}); & \Delta G > 0, \\ 1 & \Delta G \leq 0, \end{cases} \tag{9}$$

where ΔG is the change in energy caused by the change of orientation and k_b is the Boltzman constant. Successful transitions at the grain boundaries to orientations of nearest neighbor grains corresponds to boundary migration. A segment of boundary, therefore, moves with a velocity related to the local chemical potential difference, ΔG_i, by:

$$v_i = C[1 - \exp(-\Delta G_i / k_b \mathbf{T})]. \tag{10}$$

The prefactor C has a sense of boundary mobility.

It was concluded in [19] that *for two-dimensional* lattice grain growth exponent p (p=1/n) depends on temperature and number L of possible grain orientations in

lattice. The grain growth exponent decreases from 0.5 to 0.4 with L increase, the p=0.4 was found as the limit for $L\to\infty$. It was shown, that this is in reasonable agreement with isothermal grain growth experiments on zone refined metals. However, the maximum L in [6.3] was limited by 64 possible orientations for individual site. No attempt to control two-dimensional texture evolution on grain growth was done.

The approach developed [6.3] was taken as a basis in this study. However, modeling volume now is considered as *three-dimentional* matrix of sites. Following [6.3], each site of modeling space is assigned a number L; $0<L<180^2$, corresponding to actual crystallographic orientation of the site (whole spatial angle is divided on 32400 segments of 1×1 degree). The smallest initial grain is considered to be about 10 μm in diameter, so each site of modeling volume is 3×3×3μm and the smallest initial grain consists from 35-40 sites of modeling volume. Modeling volume has a cubic shape and includes 180^3 sites (540^3μm). This is equivalent to about 163600 grains within the modeling volume in initial state. Each grain is characterized by grain volume (i.e. by number of sites having the same orientation L in a given cluster). The time unit is the "1 MC run" which means that the number of single trial procedures done in accordance to (10, 11) is equal to the number of sites in modeling volume.

The model allows:

1) to divide the modeling volume into clusters having grain-like shape and a given average initial size;
2) to employ a model texture into the model volume by assigning the appropriate L value to each site of modeling volume;
3) to employ the $M_{ij}(\varphi)$ factor to (9), that represents the intergranular boundary mobility as the function of angle between the main crystallographic directions of two neighborhood grains:

$$W=\begin{cases} M_{ij}\exp(-\Delta G/k_b\mathbf{T}); & \Delta G>0, \\ 1 & \Delta G\le 0, \end{cases} \qquad (11)$$

4) to reconstruct actual texture of modeling volume after each MC run;
5) to build the images (sections) of the modeling volume for the visualization of the grain structure (each orientation corresponds to single color) after each MC run;
6) to determine an average grain size and total number of grains in the modeling volume.

As the first approximation, $M_{ij}(\varphi)$ factor was taken from [6.4] as that for tilt boundaries in cubic lattices formed by symmetric rotations of the grains around a common [100] axis (Figure 6.1).

Two modeling experiments were performed so far:

1. Initially not textured state, $M_{ij}(\varphi)$=1 control procedure to verify the validity of software.
2. Initial two-component texture (Figure 6.2) with integral intensities ratio 1/2 (I_c/I_{45} = 2.0/1.0), $M_{ij}(\varphi)$ as on Figure 6.1.

As it was expected, the first experiment did not show any textural changes during the grain growth which itself follows the normal kinetics with n = 4. Figure 6.3 presents sections of modeling volume for different "annealing" times: the evolution of grain structure is clearly seen.

Some results of second experiment are presented in Figure 6.4. Normal grain growth started with n = 3.8 and remained relatively fast during the interchange of intensities between two textural components. After 100 MC runs n increased up to 14-16 (i.e. a lot grain boundaries having low mobility appeared in modeling volume). It is supposed that after the slow growing grains will become big enough to interact with each other, the grain growth will again become faster. Verifying this is in progress; supposedly this will happen after 2000 MC runs.

The preliminary experiments showed that model developed is able to simulate the grain growth in textured materials. Further development of the model would help in better understanding of the beta grain growth mechanism in titanium alloys.

References.

6.1. Kim B.N. Two-dimentional simulation of grain growth based on atomic jump model for grain boundary migration. Mat. Sci. and Eng. V. A283, 2000, pp. 164-171.

6.2. Wakai F., Enomoto N. and Ogawa H. Three-dimensional microstructural evolution in ideal grain growth-general statistics. Acta mater., v. 48, 2000, pp. 1297-1311.

6.3. Anderson M.P., Srolovitz D.G., Grest G.S. and Sahni P.S. Computer simulation of grain growth I. Kinetics. Acta metall. v. 32, 1984, pp. 784-791.

6.4. Shewmon P.G. Energy and Structure of Grain Boundaries. In Recrystalization, Grain Growth and Textures. Papers presented at a Seminar of ASM, 1965, pp. 165-202.

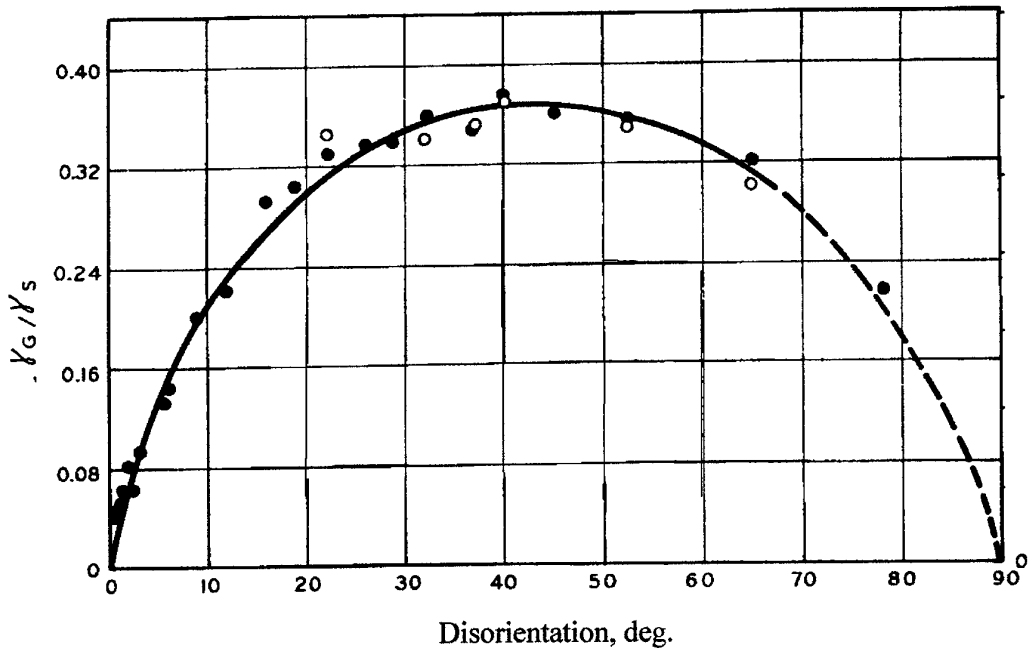

Figure 6.1. Normalized factor $M_{ij}(\varphi)$ for tilt boundaries in cubic lattices formed by symmetric rotations of the grains around a common [100] axis [6.4].

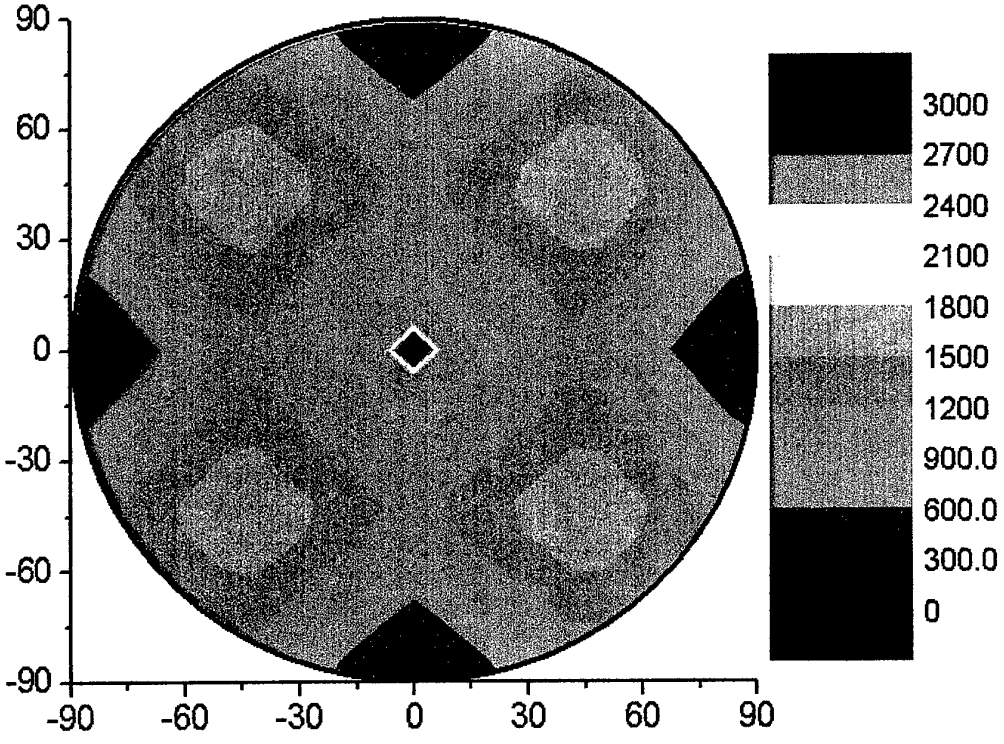

Figure 6.2. Initial two-component texture with integral intensities ratio 1/2.

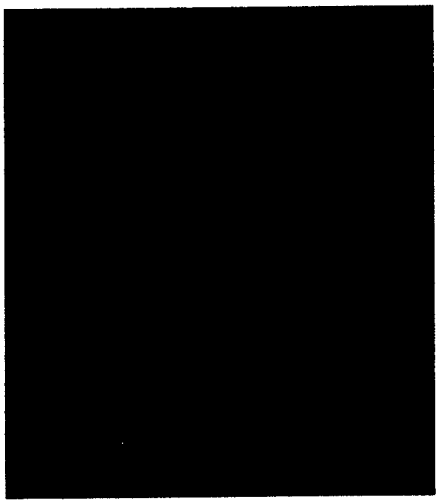

6 MC runs, $D = 21.42$ μm

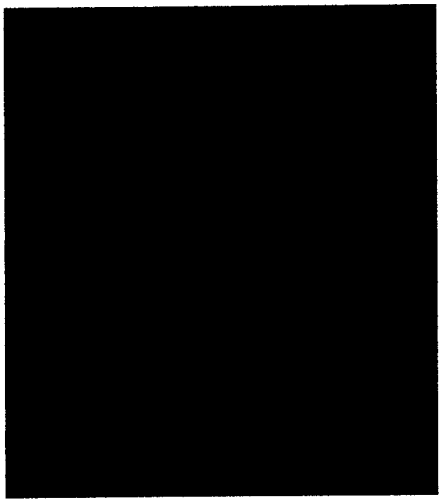

15 MC runs, $D = 26.18$ μm

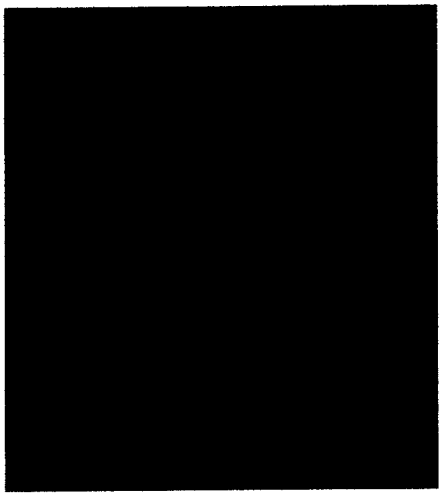

50 MC runs, $D = 34.38$ μm

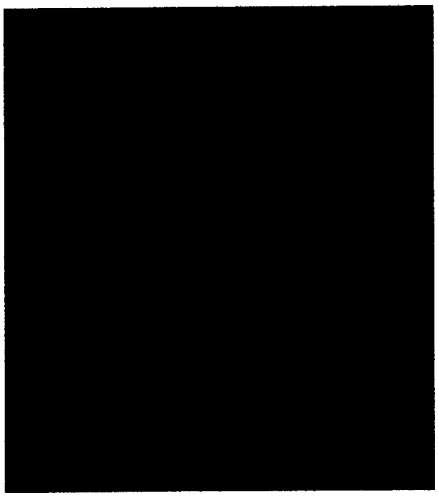

100 MC runs, $D = 42.67$ μm

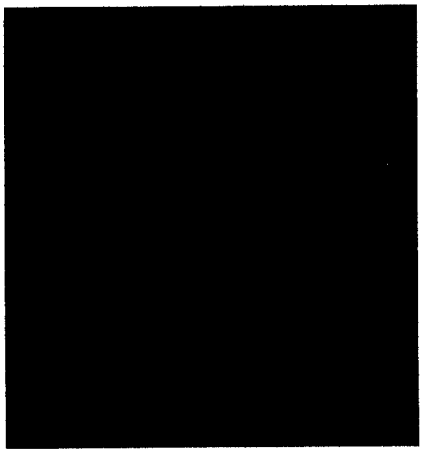

180 MC runs, $D = 50.20$ μm

Figure 6.3. Sections of modeling volume for different "annealing times" in initially not textured material, $M_{ij}(\varphi)$=1.

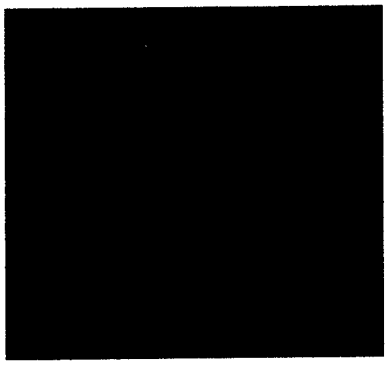

0 MC runs, $D = 12.00$ μm

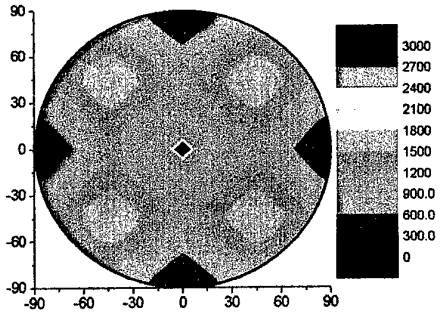

$I_c/I_{45} = 2/1$

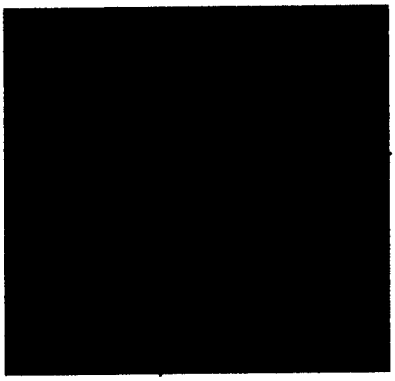

5 MC runs, $D = 16.32$ μm

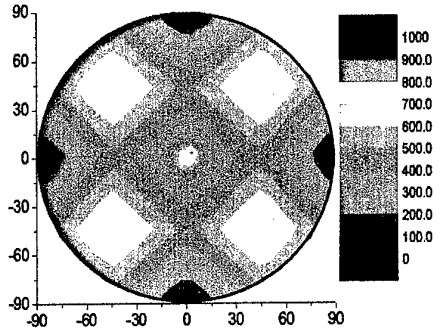

$I_c/I_{45} = 1.2/1.0$

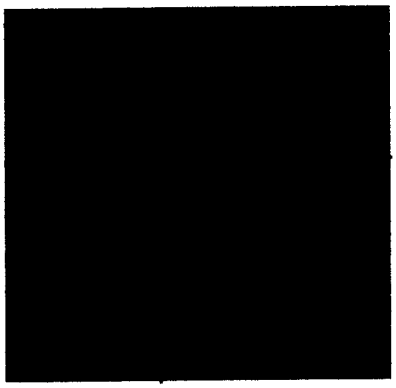

10 MC runs, $D = 28.38$ μm

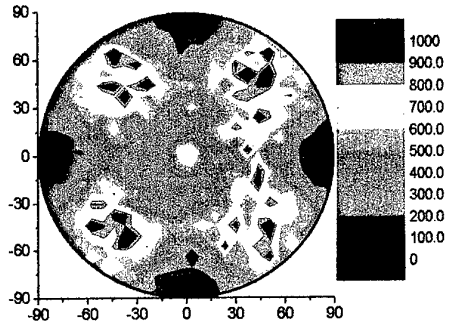

$I_c/I_{45} = 1/2.7$

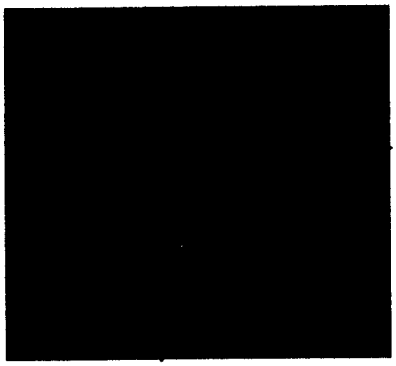

80 MC runs, $D = 46.52$ μm

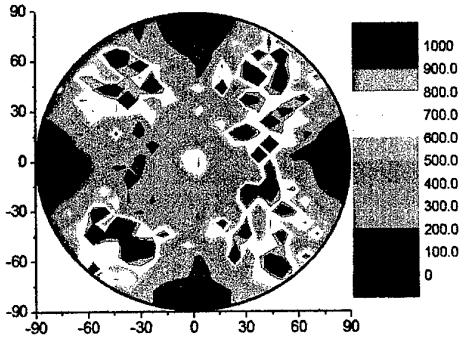

$I_c/I_{45} = 1/8.7$

Figure 6.4. Sections of modeling volume for different "annealing times" in initially textured material, $M_{ij}(\varphi)$ is of type as on Figure 6.1.

7. Conclusions

1. Numerous experimental data on beta grain growth in Ti6Al-4V during both rapid, continuos and isothermal heat treatments were received.
2. It was shown quite conclusively that beta grain growth is strongly affected by initial texture and its evolution during heating. This leads to a dramatic difference in a final beta grain microstructure in a chemically and morphologically identical materials which have different initial textures. On the other hand, it requires the strict control of texture to be imposed in thermomechanical processing and heat treatments of titanium alloys to ensure the desired level of those mechanical properties which are affected by the beta grain size.
3. Beta grain growth kinetics in textured Ti-6Al-4V are found to be of discontinuous type; stages of fast and slow growth alternate. The alternation is explained by cyclic texture evolution: fast and slow growth the time periods when material is in a textured or randomized conditions respectively.
4. Simulation of texture influenced grain growth using Monte-Carlo technique has been initiated.
5. Focus of future research efforts in this field should be on (a) development of simulation technique for last to be able to explain the experimental data available and (b) further experiments on solute rich titanium alloys with lower beta transus temperatures than in Ti-6Al-4V and higher volume fractions of beta phase in the initial condition. Such alloys would have generally smaller initial grain sizes and enable the determination of beta-grain growth at lower temperatures and over a wider temperature interval. Moreover, texture evolution would be evaluated not only in beta but also in the two-phase alpha + beta field as well. Taken together, this fundamental research would lead to a more precise understanding of the interrelation of texture evolution and beta grain growth.